Journal of Medicinal Chemistry

Article

pubs.acs.org/jmc

Identification of Novel HSP90α/β Isoform Selective Inhibitors Using Structure-Based Drug Design. Demonstration of Potential Utility in Treating CNS Disorders such as Huntington's Disease

Justin T. Ernst,*[,†] Timothy Neubert,[†] Michael Liu,[†] Samuel Sperry,[†] Harmon Zuccola,[‡] Amy Turnbull,[†] Beth Fleck,[†] William Kargo,[†] Lisa Woody,[†] Peggy Chiang,[†] Dao Tran,[†] Weichao Chen,[†] Phillip Snyder,[‡] Timothy Alcacio,[†] Azin Nezami,[‡] James Reynolds,[†] Khisal Alvi,[†] Lance Goulet,[†] and Dean Stamos[†]

[†]Vertex Pharmaceuticals, 11010 Torreyana Road, San Diego, California 92121, United States

[‡]Vertex Pharmaceuticals, 130 Waverly Street, Cambridge, Massachusetts 02139, United States

Supporting Information

ABSTRACT: A structure-based drug design strategy was used to optimize a novel benzolactam series of HSP90α/β inhibitors to achieve >1000-fold selectivity versus the HSP90 endoplasmic reticulum and mitochondrial isoforms (GRP94 and TRAP1, respectively). Selective HSP90α/β inhibitors were found to be equipotent to pan-HSP90 inhibitors in promoting the clearance of mutant huntingtin protein (mHtt) in vitro, however with less cellular toxicity. Improved tolerability profiles may enable the use of HSP90α/β selective inhibitors in treating chronic neurodegenerative indications such as Huntington's disease (HD). A potent, selective, orally available HSP90α/β inhibitor was identified (compound **31**) that crosses the blood−brain barrier. Compound **31** demonstrated proof of concept by successfully reducing brain Htt levels following oral dosing in rats.

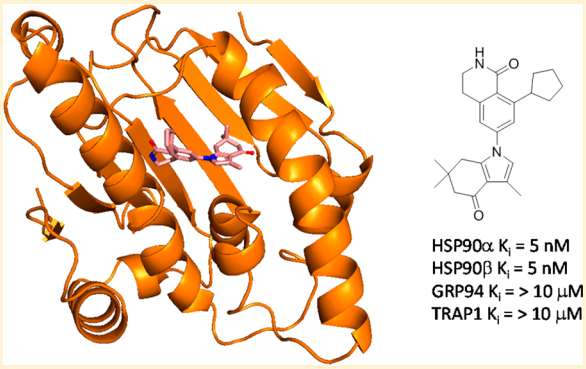

INTRODUCTION

HSP90 is a molecular chaperone that is responsible for the proper folding of multiple client proteins.[1] Numerous small molecule HSP90 inhibitor programs have been disclosed in the literature and have been reviewed extensively.[2] The majority of these programs have targeted the ATP-binding site of the N-terminal domain, which regulates the turnover of folded client proteins.[3] All of the HSP90 inhibitors that have entered clinical trials bind to this site, and to date these studies have been primarily focused on treating oncology indications.[2] The use of HSP90 inhibitors outside of oncology has been limited, due predominately to modest tolerability profiles. We have recently disclosed a strategy to decrease mechanism-based toxicities associated with inhibiting HSP90.[4] This strategy involves selectively targeting the cytosolic isoforms of HSP90 (inducible α and constitutive β) versus the mitochondria (HSP75/TRAP1) and endoplasmic reticulum (GRP94) isoforms. This approach reduces the number of client proteins affected and retains the functions of GRP94 and TRAP1, which have been shown to be essential for ER and mitochondrial viability, respectively.[5]

Mutant and wild-type Huntingtin (Htt) have been reported to be client proteins of HSP90, therefore, inhibition of HSP90 (via inhibiting N-terminal ATP-ase activity) results in degradation of these proteins via the proteosome.[6] Mutant Htt is the toxic species that is responsible for Huntington's disease,[7] thus decreasing levels of this protein in the CNS of patients carrying a copy of the mutant allele should reduce or eliminate disease progression. Selective siRNA knockdown of the cytosolic forms of HSP90 (α and β) is sufficient to promote the degradation of mutant Huntingtin (mHtt).[4] On the basis of these data, we initiated a structure-based drug design strategy to identify novel, brain penetrating HSP90α/β isoform selective inhibitors for treating HD and potentially other neurodegenerative disorders.

In a recent publication, we described the correlation between chemotype-dependent binding conformations of HSP90α/β and isoform selectivity.[4] Several published inhibitors, such as **1** (SNX-0723),[8] possess a modest level of HSP90α/β isoform selectivity. The molecular basis for this selectivity is hypothesized to be driven by the stabilization of an extended α-helical conformation in the residue 104−111 region of HSP90α/β (Figure 1A).[4] This conformation is believed to be less energetically favorable or not accessible in the case of binding GRP94 and TRAP1. Compounds such as **2** (AUY-922),[9] which have little to no isoform selectivity, do not strongly interact with this region of the HSP90 isoforms (Figure 1B). Thus, for chemical series such as the benzamide-tetrahydroindolones (i.e., **1**), a significant level of isoform

Received: January 8, 2014
Published: March 27, 2014

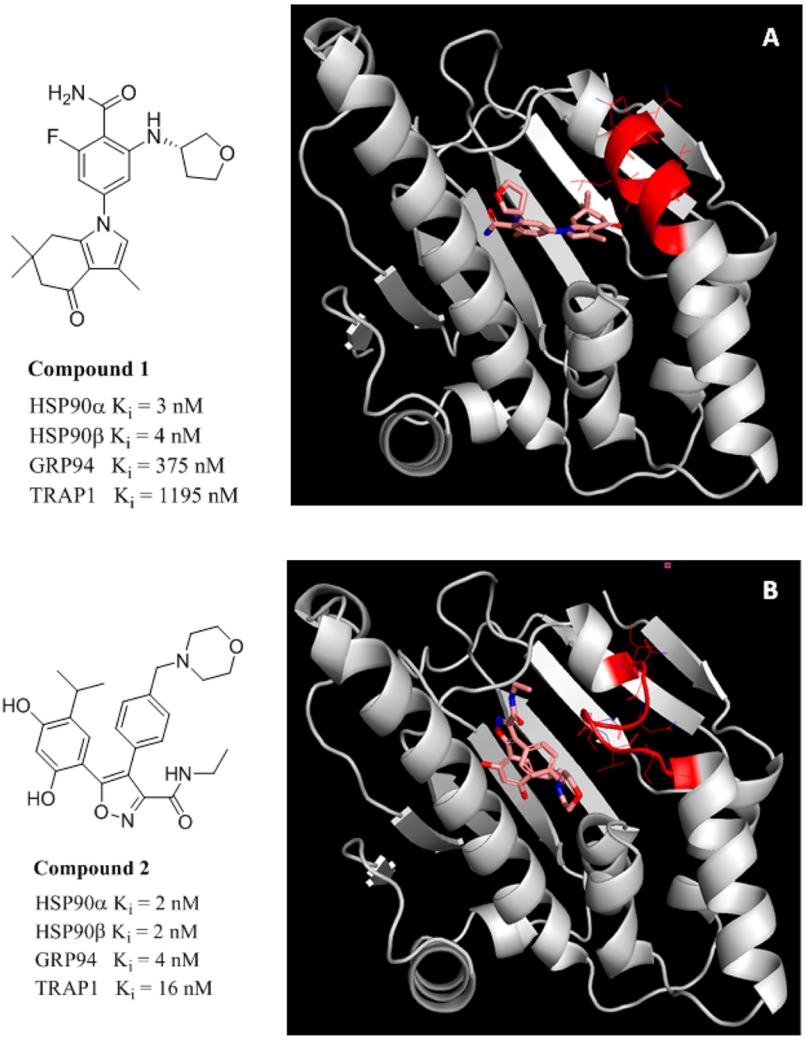

Figure 1. Isoform selectivity profiles and X-ray structures of compounds **1** ((A) PDB code 4NH8) and **2** ((B) PDB code 2VCI) bound to the N-terminal domain of HSP90*α*. Residues 104−111 of HSP90*α* are highlighted in red.

selectivity is obtainable from taking advantage of conformational aspects of inhibitor binding modes versus residue differences in the binding pockets of the four isoforms.

RESULTS AND DISCUSSION

The fact that compound **1** possesses some degree of selectivity versus GRP94 and TRAP1 and was reported to be CNS penetrating[8] made this compound an attractive starting point for further optimization. Thus, the main objective of our approach was to further improve isoform selectivity (K_i values for GRP94 and TRAP1 > 10 μM) while optimizing cellular potency (mHtt clearance) and CNS exposure profiles. An additional goal was to identify novel chemical matter through the optimization process. An analysis of the binding mode of **1** to HSP90*α* (Figure 2) indicates that the 3-methylpyrrole portion of the tetrahydroindolone core is directed toward the helical residues 104−111. Given the impact of this region of the protein on isoform selectivity properties, a set of analogues utilizing novel tricyclic-tetrahydroindolone motifs was prepared (analogues **4**−**10** in Table 1), thus expanding the part of the scaffold directed toward the residue 104−111 helix. These systems were chosen primarily in an attempt to maximize the fit into a hydrophobic cleft formed by residues I110, A111, and V136. In some cases, polar groups were incorporated to probe

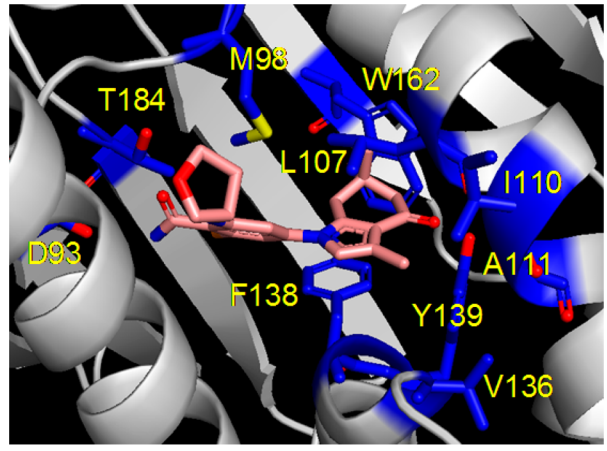

Figure 2. Binding mode of compound **1** (PDB code 4NH8). The key binding residues of HSP90*α* are highlighted in blue.

for additional interactions with backbone hydrogen bonding groups or water molecules at the solvent interface.

The N-Me octahydro-*β*-carboline analogue **8** was identified from this set as a suitable starting point for further optimization, although overall the approach failed to yield a

dx.doi.org/10.1021/jm500042s | J. Med. Chem. 2014, 57, 3382−3400

Table 1. SAR Studies for Benzamide-tetrahydroindolone Analogues

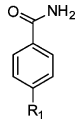

	R1	HSP90α K_i (μM)[a]	HSP90β K_i (μM)[a]	GRP94 K_i (μM)[a]	TRAP1 K_i (μM)[a]
3	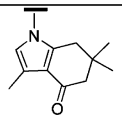	0.23 ± 0.03	0.21 ± 0.04	>10.0	8.7 ± 3.6
4	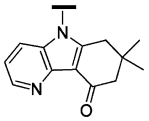	>10.0	>10.0	>10.0	>10.0
5	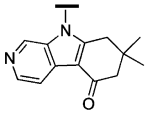	>10.0	>10.0	>10.0	>10.0
6	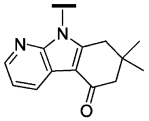	2.5 ± 0.24	2.6 ± 0.54	>10.0	>10.0
7	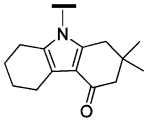	3.2 ± 0.25	2.9 ± 0.26	>10.0	>10.0
8	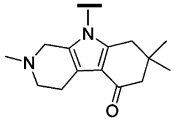	0.69 ± 0.13	0.58 ± 0.13	>10.0	>10.0
9	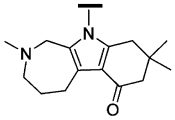	>10.0	>10.0	>10.0	>10.0
10	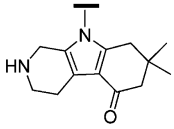	1.9 ± 0.37	1.5 ± 0.15	>10.0	>10.0

[a]Values were determined using fluorescence polarization-based binding assays.

scaffold with improved HSP90α/β binding affinities versus the parent tetrahydroindolone structure **3**.[10] The basicity of **8** (pK_a = 7.6), however, was deemed to be attractive because many HSP90 inhibitors, including the benzamide-tetrahydroindolone series (i.e., **3**), suffer from poor aqueous solubility. The inactivity of the 7-membered N-Me β-carboline analogue **9** along with reduced binding affinity for the cyclohexene derivative **7** suggested that the N-Me moiety in **8** is forming a specific interaction in the active sites of HSP90α/β. Because compound **8** has similar potency to tetrahydroindolone **3**, this interaction was thought to offset energetic penalties due to the incorporation of the additional ring system. An X-ray structure was obtained for compound **8** bound to HSP90α. The structure indicated that a hydrogen bond mediated by a water molecule is present between the basic center of the octahydro-β-carboline and N51 (Figure 3A). Also, the piperidine ring occupies the hydrophobic cleft formed in part by helix 104−111 as designed (Figure 3B). Comparing the X-ray structures for **1** and compound **8** bound to HSP90α revealed that the binding modes of the benzamide-tetrahydroindolone systems are highly conserved (Figure 3C). As expected, incorporation of the analogous benzamide functionality of **1** into **8** resulted in a 20-fold increase in HSP90α/β binding affinities (compound **11** in Table 2). However, increases in GRP94 and TRAP1 binding affinities were also observed. Comparing the isoform selectivity ratios of **1** and **11** indicated that the additional piperidine ring was unsuccessful in improving this property despite forming additional interactions with helix 104−111. Therefore, it was deemed that a different approach would ultimately have to be employed to further increase the isoform selectivity of this system.

dx.doi.org/10.1021/jm500042s | J. Med. Chem. 2014, 57, 3382−3400

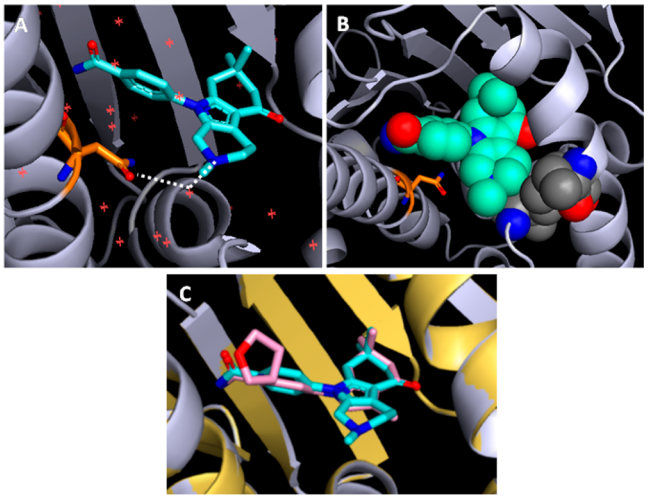

Figure 3. X-ray structure of **8** (blue) bound to HSP90α (gray ribbon), PDB code 4O04: (A) hydrogen bonding highlighted from basic nitrogen to N51 via a water molecule; (B) spacefill model of **8** highlighting the fit of the piperidine system into a hydrophobic pocket formed by I110, A111, and V136; (C) overlap of the X-ray structures for **8** and **1** (pink, HSP90α is yellow ribbon).

Compound **11** was tested in a cellular assay to determine the effects on mHtt clearance and was found to be moderately potent. Removal of the fluorine substituent (compound **12**) appeared to have little effect on cellular potency and isoform selectivity. A focused set of compounds was prepared at this point to explore the effects of aniline substitution on isoform selectivity and cellular potency (**13**–**22**). Although a large, diverse set of side chains was tolerated at this position, this approach did not lead to the identification of a system that was both highly potent for mHtt clearance (IC_{50} mHtt < 50 nM) and isoform selective (K_i values for GRP94 and TRAP1 > 10 μM).

An analysis of the X-ray structures of HSP90α and GRP94 bound to **1** revealed that there was a subtle amino acid difference in the active sites adjacent to the benzamide moiety that could offer the opportunity to further modulate isoform selectivity (Figure 4).[4] In the case of HSP90α and β, residue 186 is a valine. The analogous residue in GRP94 and TRAP1 is an isoleucine, thus providing slightly increased steric bulk at this position (Figure 4A). Analysis of the GRP94-bound structure of **1** revealed that there is a tight fit for this isoleucine and the fluorine substituent of the benzamide (Figure 4B). It was hypothesized that optimization of benzylic substitution *ortho* to the primary amide could maximize the fit with V186 in the case of HSP90α/β but sterically clash with the extra methyl of the analogous isoleucine residue in GRP94 and TRAP1. To ensure benzylic substitution would not adversely affect the orientation of the primary amide for optimal hydrogen bonding, cyclization of this position to the amide was envisioned to rigidify the system. This strategy offered the advantages of removing an unneeded hydrogen bond donor of the primary amide and reducing the overall PSA of the scaffold, thus improving the physicochemical properties of the system to favor CNS penetration. In addition, it was deemed that the resulting lactam structures further contributed to the novelty of the chemical series. In fact, previously reported SAR studies suggested that secondary amides were not tolerated at this position,[10] although in these cases the amides were acyclic and presumably would adopt conformations less ideal for optimal hydrogen bonding in the active site.

To test this hypothesis, benzolactam **23** was prepared (Table 3). Lactam **23** has similar HSP90α/β binding affinities compared to primary amide **21** but has improved isoform selectivity and cellular potency. The X-ray structure of **23** with HSP90α confirmed the predicted binding mode, with the benzylic methylene of the lactam fitting tightly with the side chain of V186 (Figure 5A). Also, the orientation of the lactam hydrogen bond donor/acceptor pair is identical to that observed in the case of the primary amide system (Figure 5B). To better understand the flexibility of the lactam system, analogues **24**–**26** were prepared. The data for these analogues clearly indicate the sensitive nature of the hydrogen bond donor/acceptor pair, with both the 5- and 7-membered lactam systems being inactive compared to 6-membered lactam **25**.

Given the rigidification of the hydrogen bond donor/acceptor system in the lactam, replacement of the *ortho* aniline side chain in **23** with a carbon linked side chain was examined. In the primary amide-based systems (i.e., **14**), the N–H of the aniline side chain forms an intramolecular hydrogen bond to the carbonyl of the amide. This intramolecular hydrogen bond is needed to reduce the free rotation of the amide and accounts for as much as a 20-fold increase in HSP90α/β binding affinity (comparing **14** with **27**). However, in the case of the lactam system, it was hypothesized that the requirement for the intramolecular hydrogen bonding was no longer necessary. Replacement of the aniline was viewed as advantageous because it eliminates a potential genotoxic risk factor and further improves the CNS lead-like properties of the system by removing a hydrogen bond donor and reducing PSA. Compound **28** was prepared and was found to have very similar potency and isoform selectivity properties compared to the analogous aniline analogue **23**. Comparing the X-ray structures of **23** and **28** bound to HSP90α revealed that the binding modes of the two inhibitors are well conserved, with the exception of the alkyl side chains which adopt different poses (Figure 6). Removal of the aniline moiety results in increased conformational mobility of the alkyl side chain due to loss of the intramolecular hydrogen bond, however, this increased flexibility has little impact on the HSP90α/β binding affinities and isoform selectivity.

Compound **28** was evaluated in human HD patient derived fibroblasts for its effects on HSP90 client protein levels and HSP70 induction (Figure 7). Dose dependent reductions were observed for Htt (IC_{50} = 27 nM) as well as client proteins CDK4 and AKT. Also, increases in HSP70 were clearly observed at concentrations of **28** that produced client protein clearance, consistent with the mechanism of inhibiting HSP90α/β.

The pharmacokinetic properties of compound **28** were evaluated in rats using subcutaneous and intravenous delivery (Table 4). Compound **28** suffers from high plasma clearance and limited brain exposure. Evaluation of **28** in a MDR1-MDCK permeability assay[11] indicated that it was a P-gp efflux substrate because the ratio of basal-to-apical permeability to apical-to-basal permeability (BA/AB) is 42. This property is most likely the key driver of the observed poor brain to plasma ratio. SAR studies indicated that the basic amine functionality was a major contributor to the scaffold being an efflux substrate (data not shown). In addition, in vitro metabolite identification studies using human liver microsomes indicated rapid turnover due to oxidation of the piperidine ring system. These data

dx.doi.org/10.1021/jm500042s | J. Med. Chem. 2014, 57, 3382–3400

Table 2. Aniline SAR Studies in the Octahydro-β-carboline Series

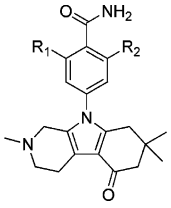

	R1	R2	HSP90α K_i (μM)[a]	HSP90β K_i (μM)[a]	GRP94 K_i (μM)[a]	TRAP1 K_i (μM)[a]	mHtt IC_{50} (μM)[b]
11	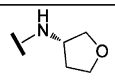	F	0.032 ± 0.010	0.031 ± 0.009	4.4 ± 0.9	8.5 ± 1.9	0.12 ± 0.06
12	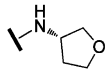	H	0.042 ± 0.011	0.035 ± 0.009	1.1 ± 0.5	5.0 ± 1.3	0.12 ± 0.03
13	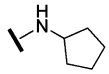	H	0.014 ± 0.005	0.012 ± 0.005	0.58 ± 0.15	1.7 ± 0.5	0.11 ± 0.04
14	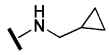	H	0.017 ± 0.003	0.019 ± 0.004	2.8 ± 0.9	4.5 ± 1.0	0.19 ± 0.08
15	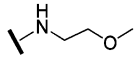	H	0.062 ± 0.014	0.060 ± 0.008	>10.0	8.8 ± 3.8	0.72 ± 0.23
16	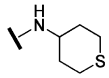	H	0.028 ± 0.011	0.025 ± 0.009	0.42 ± 0.07	1.2 ± 0.3	0.09 ± 0.03
17	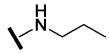	H	0.022 ± 0.005	0.021 ± 0.004	3.2 ± 1.2	5.8 ± 1.5	0.19 ± 0.08
18		H	0.046 ± 0.011	0.048 ± 0.009	>10.0	>10.0	0.42 ± 0.13
19	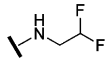	H	0.028 ± 0.010	0.029 ± 0.010	3.7 ± 1.2	7.4 ± 1.0	0.22 ± 0.09
20	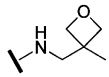	H	0.028 ± 0.006	0.022 ± 0.003	0.62 ± 0.09	1.2 ± 0.1	0.45 ± 0.24
21		H	0.025 ± 0.007	0.025 ± 0.008	2.9 ± 1.0	>10.0	0.14 ± 0.06
22	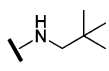	H	0.022 ± 0.004	0.022 ± 0.002	0.84 ± 0.13	1.4 ± 0.4	0.93 ± 0.10

[a]Values were determined using fluorescence polarization-based binding assays. [b]Values were derived from an in-cell western assay for mHtt in HEK cells.

suggested that the piperidine ring was a liability for both efflux and metabolic stability, and thus it was decided that removal of the basic system was necessary. The disadvantages of this strategy were that aqueous solubility and cellular potency properties could be compromised. Previous SAR studies (i.e., comparison of **12** and **29** in Figure 8) indicated that the basic systems generally had greater aqueous solubility and cellular potency versus nonbasic systems with similar HSP90α/β binding affinities.

It was decided to revisit the 3-methyl tetrahydroindolone system as a replacement for the octahydro-β-carboline moiety in the benzolactam series (compound **30** in Table 5).

dx.doi.org/10.1021/jm500042s | J. Med. Chem. 2014, 57, 3382−3400

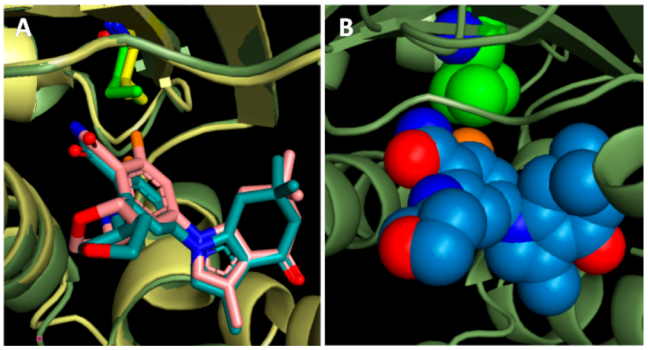

Figure 4. (A) Overlap of the X-ray structures of **1** (pink) bound to HSP90α (yellow ribbon, V186 highlighted in yellow) and **1** (blue) bound to GRP94 (green ribbon, isoleucine at analogous position to V186 highlighted in green), PDB code 4NH9; (B) X-ray structure of **1** (blue spacefill model, benzylic F in orange) bound to GRP94 (green ribbon, key isoleucine highlighted as green spacefill model).

Fortunately, in this case, the potency and selectivity profiles of **30** were found to be quite similar to **28**, although the aqueous solubility, as predicted, was much reduced (4 μM versus 122 μM for **28**). The rat pharmacokinetic properties of **30** are shown in Table 4. Overall, a 5-fold improvement in brain exposure was observed versus compound **28**. Evaluation of **30** in the MDR1-MDCK permeability system indicated that removal of the basic ring successfully mitigated the efflux liability (BA/AB = 1) and is most likely the reason for the observed increase in the brain to plasma ratio. Also, as predicted, removal of the piperidine ring system resulted in reduced plasma clearance.

Given the attractive CNS exposure properties of **30**, further SAR studies were conducted within the lactam−tetrahydroindolone system in an attempt to improve cellular potency while maintaining good PK and isoform selectivity properties. Substitution *ortho* to the amide system was once again revisited due to the precedented flexibility at this position. Also, an analysis of the X-ray structure of **30** bound to HSP90α (Figure 9A) indicated that substitution at this position could be used to "shield" the amide hydrogen bond donor/acceptor system from solvent and lower the dielectric constant in this part of the binding pocket.[12] In theory, this could result in increased binding affinity by strengthening the existing hydrogen bonds to D93 and T184. A series of analogues was prepared with carbon linked substitution *ortho* to the lactam. From these studies, the cyclopentyl analogue **31** was identified as having excellent HSP90α/β binding affinities, cellular potency, and isoform selectivity properties (Table 5).

An X-ray structure of **31** bound to HSP90α was obtained (Figure 9B) and indicated that the cyclopentane side chain completely blocks access of solvent to the hydrogen bond donor/acceptor system of the lactam. Furthermore, ITC measurements for the binding of **30** and **31** to HSP90α indicated that the difference in binding affinities was due to a 1.6 kcal/mol increase in binding enthalpy for **31**. Both of these results are consistent with the "shielding" hypothesis.

With compound **31** identified, a set of studies was conducted to probe whether isoform selectivity versus GRP94 and TRAP1 translates into reduced cytotoxicity in vitro. Compounds **31**, **1**, and **2** were tested in an HD-patient fibroblast cell system for mHtt reduction and cytotoxicity (Table 6). These three compounds represent varying degrees of isoform selectivity. Compound **31**, which shows no measurable binding affinity to GRP94 and TRAP1, has a >100-fold window between the IC_{50} for mHtt clearance (6 nM) and the CC_{50} for cytotoxicity (>10 μM). Compound **1**, which has modest selectivity, has a much reduced CC_{50}/IC_{50} mHtt ratio (ratio = 4) compared to **31**. Finally, for **2**, which has little to no isoform selectivity, the CC_{50}/IC_{50} mHtt ratio is essentially one. Overall, these data support the hypothesis that HSP90α/β isoform selective inhibitors are equally efficacious for Htt clearance and less cytotoxic versus pan-HSP90 inhibitors.

Compound **31** was progressed into rat PK/PD studies to assess its effects on Htt concentrations in brain tissue. It has been previously shown that the HSP90-mediated clearance of Htt protein is nonselective for mutant forms of the protein versus wild-type Htt.[6] Therefore, our initial proof of concept studies were carried out in nontransgenic rats using wild-type Htt as the biomarker for efficacy. The rat PK properties of **31** are shown in Table 7. Compound **31** is orally available and successfully crosses the blood−brain barrier. A 5 mg/kg po dose given once a day for 1 week was well tolerated and successfully reduced brain Htt levels by > 50% (Figure 10). These data provide the first in vivo proof of concept demonstrating that selective HSP90α/β inhibition with a small molecule can affect brain Htt levels. Overall, these results support the continued study of the HSP90α/β-mediated reduction of Htt protein levels as a strategy to treat HD.

SYNTHETIC CHEMISTRY

The synthesis of compound **3** was previously reported.[10] Analogues **4**−**10** were prepared using similar methodology. The corresponding tetrahydroindolone systems **42** were treated with NaH in DMF and then coupled with 4-fluorocyanobenzene under high temperature. Hydrolysis of the nitrile intermediates **43** with NaOH and H_2O_2 in a mixture of EtOH and DMSO yielded the desired benzamide products (Scheme 1).

The aza-tetrahydrocarbazolone systems **50**−**52**, needed for the preparation of products **4**−**6**, were synthesized from condensation of the appropriately substituted amino-halopyridines **44**−**46** with dimedone, followed by an intramolecular Heck cyclization (Scheme 2).[13]

The octahydrocarbazolone intermediate **54**, which was required for the synthesis of **7**, was synthesized using a published modified Knorr procedure.[14] Keto-oxime **53** and dimedone were heated with Zn in AcOH and H_2O to afford the desired tricyclic system (Scheme 3).

The syntheses of β-carboline systems **59**−**61**, the building blocks necessary for the preparation of analogues **8**−**10**, are shown in Scheme 4. Amino acetals **56**−**58** were combined with formaldehyde to form the corresponding imines, which were then reacted with tetrahydroindolone **55** regioselectively at the 2-position.[15] Acidic hydrolysis of the acetals resulted in cyclization to the 3-position of the tetrahydroindolone system and subsequent reduction of the olefin intermediates using catalytic hydrogenation yielded **59**−**61**. In the case of **61**, the Bn protecting group was also removed under these reduction conditions. The secondary amine of **61** was reprotected with a BOC group to yield **62** (Scheme 5), which was then used in the SNAr coupling reaction with 4-fluorocyanobenzene. Removal of the BOC group and hydrolysis of the nitrile afforded compound **10**.

Octahydro-β-carboline analogue **11** was synthesized as shown in Scheme 6. (*S*)-Tetrahydrofuran-3-amine was added to 4-cyano-3,5-difluorobromobenzene (**63**) to yield **64**.

dx.doi.org/10.1021/jm500042s | J. Med. Chem. 2014, 57, 3382−3400

Table 3. SAR Studies in the Octahydro-β-carboline Series

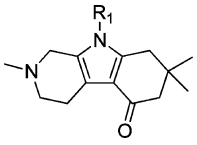

	R1	HSP90α K_i (μM)[a]	HSP90β K_i (μM)[a]	GRP94 K_i (μM)[a]	TRAP1 K_i (μM)[a]	mHtt IC_{50} (μM)[b]
23	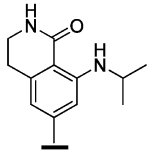	0.037 ± 0.017	0.03 ± 0.02	>10.0	>10.0	0.073 ± 0.035
24	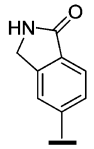	>10.0	>10.0	>10.0	>10.0	>10.0
25	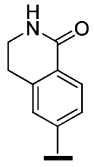	0.68 ± 0.37	0.59 ± 0.24	>10.0	>10.0	8.5 ± 3.4
26	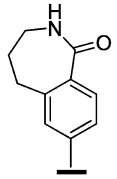	>10.0	>10.0	>10.0	>10.0	>10.0
27	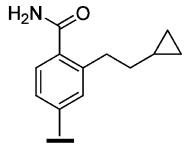	0.39 ± 0.12	0.42 ± 0.12	>10.0	>10.0	3.6
28	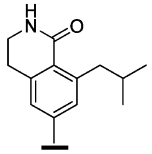	0.042 ± 0.012	0.037 ± 0.009	>10.0	>10.0	0.143 ± 0.081

[a]Values were determined using fluorescence polarization-based binding assays. [b]Values were derived from an in-cell western assay for mHtt in HEK cells.

Buchwald coupling of **64** with **59** and subsequent nitrile hydrolysis yielded compound **11**. Analogues **12**−**22** were prepared by coupling octahydro-β-carboline **59** with 3-fluoro-5-cyanobromobenzene to yield intermediate **65** (Scheme 7). Various primary amines were incorporated via Buchwald aryl amination reactions followed by nitrile hydrolyses to yield the desired compounds **12**−**22**.

Benzolactam **23** synthesis (Scheme 8) began with subjecting ketone **66** to Schmidt reaction conditions to give a mixture of lactam regioisomers which favored intermediate **67** (9:1 ratio). Isopropyl amine was coupled with **67**, with exclusive displacement of the fluorine *ortho* to the amide. Finally, an SNAr reaction with **59** yielded **23**. Lactam products **24**−**26** were prepared in one step via coupling of the commercially available fluorobenzolactams (**68**) with **59** (Scheme 9).

Two different synthetic protocols were developed to incorporate carbon linked side chains *ortho* to the primary amide (i.e., **27**) or lactam systems (**28**, **30**−**41**). The synthesis of analogue **27** is shown in Scheme 10. Suzuki coupling of 3-fluoro-5-cyanobromobenzene with (*E*)-2-(2-cyclopropylvinyl)-4,4,5,5-tetramethyl-1,3,2-dioxaborolane afforded olefin **69**. Coupling of **69** with **59**, catalytic hydrogenation of the olefin, and finally hydrolysis of the nitrile gave the desired product **27**. Lactams **28** and **30**−**41** were prepared starting from

dx.doi.org/10.1021/jm500042s | J. Med. Chem. 2014, 57, 3382−3400

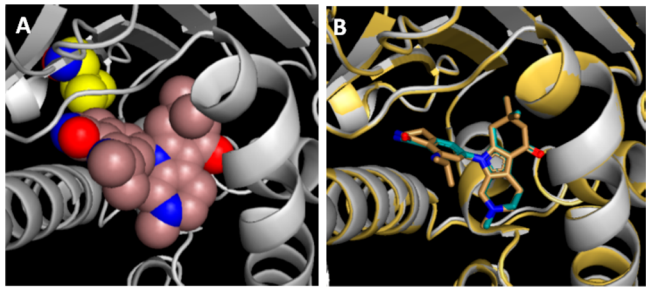

Figure 5. (A) X-ray structure of **23** (tan spacefill model) bound to HSP90α (V186 highlighted as yellow spacefill model), PDB code 4O05; (B) X-ray structure of **23** (tan) bound to HSP90α (gray ribbon) overlaid with X-ray structure of **8** bound to HSP90α (yellow ribbon).

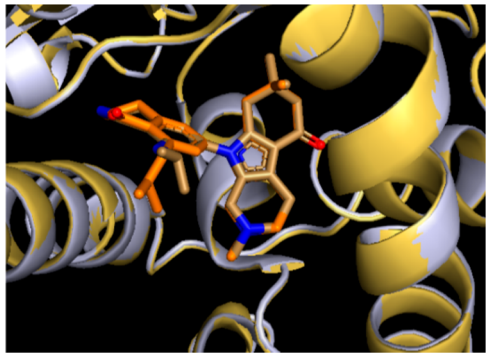

Figure 6. Overlay of X-ray structures of **23** (tan) bound to HSP90α (gray ribbon) and **28** (orange) bound to HSP90α (yellow ribbon), PDB code 4O07.

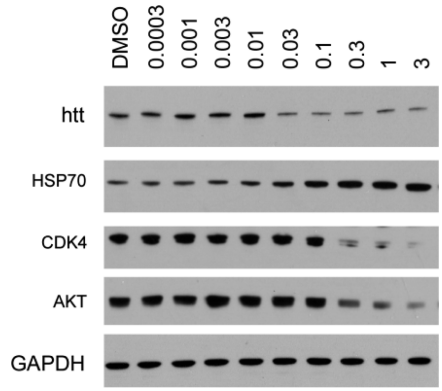

Figure 7. Effect of compound **28** (increasing concentrations in μM versus DMSO control) on HSP90 client protein and HSP70 levels in human HD patient derived fibroblasts. Proteins were quantified by Western blot and normalized to a GAPDH loading control.

difluorobenzolactam **67** (Scheme 11). Various Grignard reagents were added to **67**, and analogous to SNAr addition of amines, yielded selective displacement of the fluorine *ortho* to the amide. These intermediates (**70**) were then coupled with tetrahydroindolone **42** (where R_1 = H, R_2 = Me) under high temperature conditions to yield the desired products **28** and **30**–**41**.

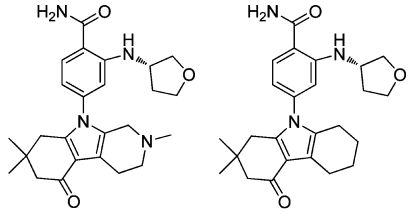

	12	**29**
K_i HSP90α/β (nM)	42, 35	36, 40
IC_{50} mHtt (nM)	120	530
Ratio IC_{50}/K_i	3	15
Aqueous solubility at pH 7.4 (μM)	> 200	27

Figure 8. Effects of basic amine functionality on solubility and cellular potency properties.

CONCLUSION

In summary, a structure-based design approach was utilized that took advantage of chemotype-dependent binding conformations, as well as a subtle amino acid difference in the active sites of HSP90α and β, to identify a novel benzolactam series with >1000-fold selectivity versus HSP90 isoforms GRP94 and TRAP1. Additional optimization, which included a hydrogen bond "shielding" strategy, resulted in the identification of compound **31**, a potent, selective, orally available HSP90α/β inhibitor with good CNS exposure. Compound **31** was found to be equipotent to pan-HSP90 inhibitors in promoting the clearance of mHtt protein in vitro, however with less cellular toxicity. Ultimately, compound **31** was used to demonstrate in vivo proof of concept by successfully reducing brain Htt levels following oral dosing in rats. Compound **31** has been advanced into further preclinical studies to probe the effects of mHtt reduction on delaying disease onset and reversing HD and other neurodegenerative phenotypes in transgenic animal models.

EXPERIMENTAL SECTION

General. All reagents and solvents were used as purchased from commercial sources. Flash column chromatography was performed with a Teledyne ISCO CombiFlash Rf system using normal-phase silica columns (230–400 mesh). ^{1}H NMR spectra were recorded on a Bruker Advance-400 spectrometer at 400 MHz or a Bruker Advance-500 spectrometer at 500 MHz. ^{13}C NMR spectra were recorded on a Bruker Advance-400 spectrometer at 100 MHz or a Bruker Advance-500 spectrometer at 125 MHz. Coupling constants (J) are expressed in hertz (Hz). Chemical shifts (δ) of NMR are reported in parts per

Table 4. Pharmacokinetic Properties of Compounds 28 and 30 in Rat

dose	AUC plasma (μg·h/mL)	Cl (mL/min/kg)	V_d (L/kg)	$T_{1/2}$ (h)	B/P (T = 2 h)
28 @ 1 mg/kg iv	0.28	57.7	7.97	2.4	
28 @ 10 mg/kg sc	2.94			7.0	0.1
30 @ 1 mg/kg iv	0.64	25.7	4.08	2.2	
30 @ 10 mg/kg sc	3.58			11.6	0.5

dx.doi.org/10.1021/jm500042s | J. Med. Chem. 2014, 57, 3382–3400

Table 5. SAR Studies in the Benzolactam−Tetrahydroindolone Series

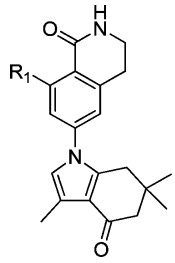

	R1	HSP90α K_i (μM)[a]	HSP90β K_i (μM)[a]	GRP94 K_i (μM)[a]	TRAP1 K_i (μM)[a]	mHtt IC_{50} (μM)[b]
30	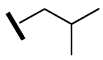	0.020 ± 0.004	0.026 ± 0.008	>10.0	>10.0	0.222 ± 0.077
31	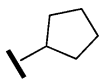	0.005 ± 0.002	0.005 ± 0.001	>10.0	>10.0	0.024 ± 0.020
32		0.006 ± 0.002	0.005 ± 0.001	>10.0	>10.0	0.036 ± 0.016
33		0.003 ± 0.002	0.003 ± 0.002	2.4 ± 1.0	>10.0	0.019 ± 0.013
34		0.034 ± 0.007	0.039 ± 0.011	>10.0	>10.0	0.195 ± 0.021
35	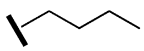	0.056 ± 0.008	0.056 ± 0.010	>10.0	>10.0	1.0
36		0.180 ± 0.035	0.140 ± 0.000	>10.0	>10.0	1.7
37	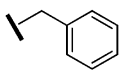	0.094 ± 0.020	0.120 ± 0.041	>10.0	>10.0	0.480 ± 0.028
38		0.014 ± 0.006	0.015 ± 0.006	>10.0	>10.0	0.230
39	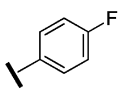	0.010 ± 0.004	0.010 ± 0.003	>10.0	>10.0	0.080 ± 0.022
40	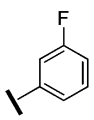	0.020 ± 0.008	0.020 ± 0.007	>10.0	>10.0	0.081 ± 0.021
41	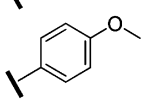	0.040 ± 0.004	0.040 ± 0.008	>10.0	>10.0	0.280

[a]Values were determined using fluorescence polarization-based binding assays. [b]Values were derived from an in-cell western assay for mHtt in HEK cells.

dx.doi.org/10.1021/jm500042s | J. Med. Chem. 2014, 57, 3382−3400

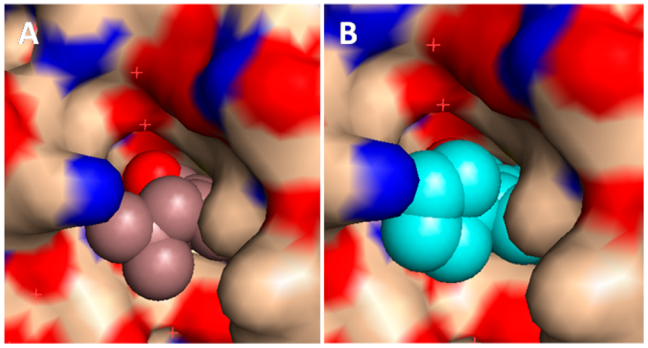

Figure 9. X-ray structures of (A) **30** (PDB code 4O09) and (B) **31** (4O0B) bound to HSP90α. The degree of lactam carbonyl "shielding" by the iBu and cyPent side chains of **30** and **31** is highlighted using space fill models. Water molecules at the edge of the binding cavity are also highlighted (red plus symbols).

Table 6. Binding Affinity, Cellular Potency, and Toxicity Properties for Compounds 31, 1, and 2

	31	1	2
K_i HSP90α (μM)[a]	0.005 ± 0.002	0.003 ± 0.002	0.002 ± 0.0001
K_i GRP94 (μM)[a]	>10.0	0.375 ± 0.022	0.004 ± 0.003
K_i TRAP1 (μM)[a]	>10.0	1.195 ± 0.090	0.016 ± 0.012
IC_{50} mHtt HD fibroblast (μM)[b]	0.006 ± 0.004	0.030 ± 0.004	0.007 ± 0.0001
CC_{50} mHtt HD fibroblast (μM)[c]	>10.0	0.140 ± 0.028	0.008 ± 0.001

[a]Values were determined using fluorescence polarization-based binding assays. [b]Values were derived from a Western blot assay for mHtt in human HD fibroblasts. [c]Viability values determined in human HD fibroblasts.

million (ppm) units relative to an internal control (TMS). Microwave reactions were performed with a Biotage Initiator focused beam microwave reactor (300 W). HPLC purification was performed on a Waters FractionLink system equipped with a Phenomenex Luna C18 column (5 μm, 75 mm × 30 mm). Analytical purity was assessed on a Waters Acquity Ultra Performance UPLC system equipped with an Acquity UPLC BEH C18 column (1.7 μm, 2.1 mm × 30 mm), and all compounds tested were determined to be >95% pure using this method. High resolution mass spectroscopy (HRMS) was performed using an Exactive Plus benchtop Oribtrap mass spectrometer connected to an UltiMate 3000 UHPLC system (Thermo Scientific). The mass spectrometer was operated in positive ionization mode. Acquisition was a full scan from m/z 150 to 1000 with a resolution of 70000.

Isothermal Calorimetry. HSP90 was extensively dialyzed against 50 mM HEPES, pH 7.5, and 100 mM NaCl, and the final dialysate was retained. Both protein and dialysis buffer were aliquoted and stored at −70 °C. Compounds were stored as 10 mM stock solutions in 100% DMSO. The DMSO stocks were diluted with the retained dialysate, and DMSO was added to the protein solution to obtain equal volume percentage of DMSO in the protein and ligand solution. All calorimetry experiments were performed in a VP-ITC instrument (GE/Microcal, Northampton, MA). For each experiment, the protein solution (100 μM in buffer) was loaded into the syringe and compound (10 μM in identical buffer) into the sample cell. This method was necessary due to the low solubility of compounds in aqueous buffer. Calorimetry experiments were performed at 25 °C, stirring at a rate of 307 RPM, with a reference power of 5 μCal s^{-1}. The HSP90 was injected consecutively (10−20 μL per injection) until the ligand in the cell reached saturation. Data were analyzed with the Origin 7.0 software package using a one-site model to estimate the enthalpy of binding and association constant.

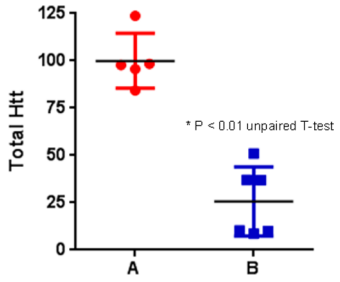

Figure 10. In vivo efficacy data (reduction of total brain Htt levels) for compound **31**; (A) rat vehicle control group (n = 5); (B) rats treated with 5 mg/kg **31** po once a day for 1 week (n = 6).

Pharmacokinetic Studies. In vivowork for the pharmacokinetic studies was performed at Vertex Pharmaceuticals (San Diego, CA). Groups of male Sprague−Dawley rats (n = 3 per dose group) were administered as single doses of **28**, **30**, or **31**. Compounds were formulated in 10% dimethylisosorbide, 15% ethanol, 35% polyethylene glycol (PEG400), and 40% dextrose (5% in water, D5W) for intravenous administration at a nominal dose level of 1 mg/kg. Compounds were formulated as suspensions in 0.5% carboxymethylcellulose and 0.5% sodium dodecylsulfate in water for oral gavage administration at a nominal dose level of 5 mg/kg. Compounds were formulated in 60% miglyol 810, 25% water, 10% dimethyl sulfoxide, and 5% Tween 80 for subcutaneous administration at a nominal dose level of 10 mg/kg. For intravenously dosed animals, blood samples (approximately 0.25 mL each) were collected via a carotid artery catheter at 0.017, 0.083, 0.17, 0.25, 0.50, 1, 2, 4, 8, 12, and 24 h post dose. For orally dosed animals, blood samples (approximately 0.25 mL each) were collected via a carotid artery catheter at 1, 2, 4, 8, 12, 24, 48, and 72 h postdose. For subcutaneously dosed animals, blood samples (approximately 0.25 mL each) were collected at 0.25, 0.5, 1, 2, 4, 8, 12, and 24 h postdose. Each blood sample was collected into a tube that was chilled and contained potassium EDTA as the anticoagulant. Plasma was separated and stored at approximately −80 °C until analysis. Animals dosed for brain distribution were euthanized at 2 h post dose and, following perfusion with heparinized saline, were decapitated and brains harvested. Brains were stored in conical tubes at approximately −80 °C until analysis. Upon thawing, whole rat brains were homogenized in three volume equivalents of water. Following protein precipitation with acetonitrile containing an internal standard, plasma and brain samples were analyzed using a liquid chromatography/tandem mass spectrometry (LC/MS/MS) method to determine the plasma and brain concentrations of **28**, **30**, and **31**. Plasma concentration versus time data were subjected to noncompartmental pharmacokinetic analysis to determine AUC, Cl, V_d, and $T_{1/2}$.

Measurement of Mutant Huntingtin Clearance in HEK Cells. mHtt protein levels were measured using an in-cell Western blot assay in HEK cell lines stably expressing the full-length mHtt Q73 gene. Stable inducible cell lines were generated using the Flp-In TRex system from Life Technologies (catalogue no. R780-07). In brief, full-length mHtt Q73 protein overexpression was induced in HEK cells with 50 nM doxycycline and treated with compounds or DMSO.

Table 7. Pharmacokinetic Properties of Compounds 31 in Rat

dose	AUC plasma (μg·h/mL)	Cl (mL/min/kg)	V_d (L/kg)	$T_{1/2}$ (h)	B/P (T = 6 h)	% F
1 mg/kg iv	0.53	32.4	3.9	1.9		
5 mg/kg po	0.87			3.1	0.6	34

dx.doi.org/10.1021/jm500042s | J. Med. Chem. 2014, 57, 3382−3400

Scheme 1. General Methodology to Construct Benzamides 3−10[a]

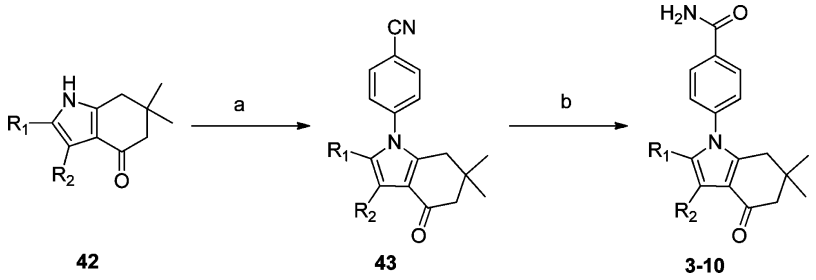

[a]Reagents and conditions: (a) NaH, 4-fluorocyanobenzene, DMF, 100−150 °C; (b) NaOH, H_2O_2, EtOH, DMSO, rt.

Scheme 2. Synthesis of aza-Tetrahydrocarbazolone Systems[a]

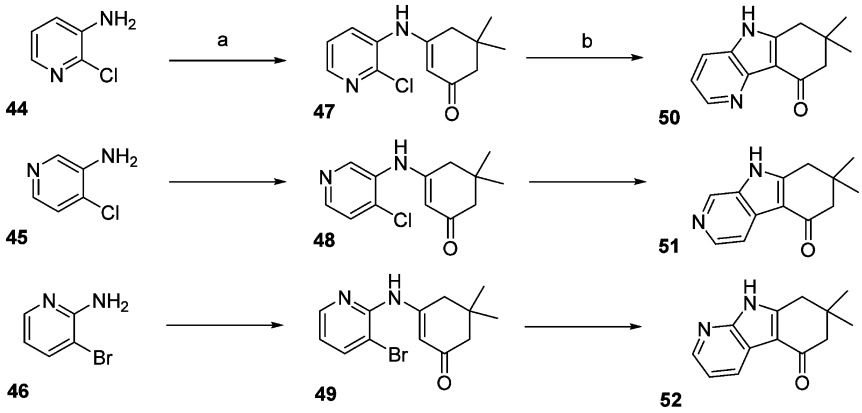

[a]Reagents and conditions: (a) dimedone, PTSA, benzene or toluene, reflux; (b) $Pd(PPh_3)_4$, Cs_2CO_3, DMF, 150 °C.

Scheme 3. Synthesis of Octahydrocarbazolone Intermediate 54[a]

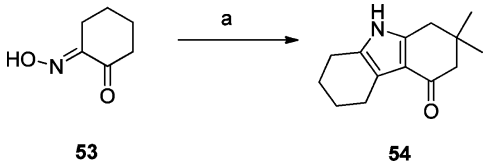

[a]Reagents and conditions: (a) dimedone, Zn, AcOH, H_2O, 80 °C.

Scheme 4. Synthesis of β-Carboline Intermediates[a]

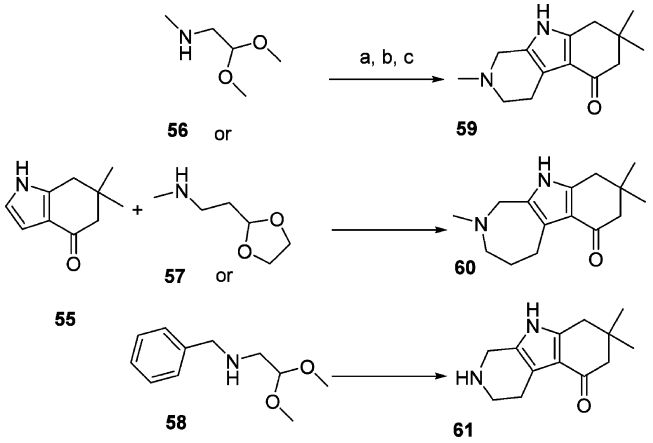

[a]Reagents and conditions: (a) formaldehyde, H_2O, AcOH, rt−75 °C; (b) 8 M HCl, 60−70 °C; (c) 10% Pd on C, EtOH, 1 atm to 30 psi H_2, rt−70 °C.

Following 24 h of incubation, cells were fixed in 10% formalin, washed, permeabilized, blocked (30 min), and stained with a Htt specific antibody (mouse monoclonal mAB2166 Millipore 1:1000 dilution) for 2 h at room temperature. Following incubation, cells were washed and incubated with a goat antimouse IRDye secondary antibody (LI-COR Biosciences) and DRAQ-5 DNA dye (for cell viability) (Biostatus Limited) diluted 1:1000 and 1:10000, respectively, in blocking buffer for 1 h at room temperature. Plates were scanned on the LI-COR Odyssey NIR Imaging system. Ratiometric analysis of Htt signal to DRAQ-5 dye was used to generate dose−response curves and IC_{50} values. IC_{50} values reported with standard deviation measurements are means of duplicate experiments.

Determination of HSP90α, HSP90β, Grp94, and Trap-1 K_i Values. K_i values were determined using a fluorescence polarization assay system. The assay was used to identify compounds that inhibit fluorescein-conjugated geldanamycin (FITC-GA) binding to the ATPase site of the HSP90 isoforms. In brief, FITC-GA was dispensed into wells containing compound for a final concentration of 5 nM FITC-GA. HSP90α, HSP90β, GRP94, or TRAP1 recombinant protein (Assay Designs, catalogue no. SPP-776, no. SPP-777, Prospec Protein Specialists, catalogue no. HSP-091) in buffer (50 mM KCl, 5 mM $MgCl_2$, 20 mM HEPES, pH 7.3−7.5, 0.1% CHAPS (Sigma C5070), 0.1% bovine gamma-globulin (Sigma G7516), and 2 mM dithiothreitol (Sigma 646563)) was then added to the well at final concentration of 10 nM. IC_{50} values were determined by measuring the amount of fluorescence polarization in the well after 2 h at varying concentrations of test compound (Perkin-Elmer Envision, 485 nm excitation, 535 nm emission, 505 nm dichroic). K_i values were calculated using the method of Nikolovska.[16] $K_i = [I]50/([L]50/K_d + [P]0/K_d + 1)$. [I]50 = concentration of free inhibitor at 50% inhibition, [L]50 = concentration of free fluorescence labeled ligand molecule at 50% inhibition, [P]0 = concentration of free protein at 0% inhibition, K_d = dissociation constant of the protein−ligand complex. All reported K_i values are means of duplicate experiments.

dx.doi.org/10.1021/jm500042s | J. Med. Chem. 2014, 57, 3382−3400

Scheme 5. Synthesis of β-Carboline Analogue 10[a]

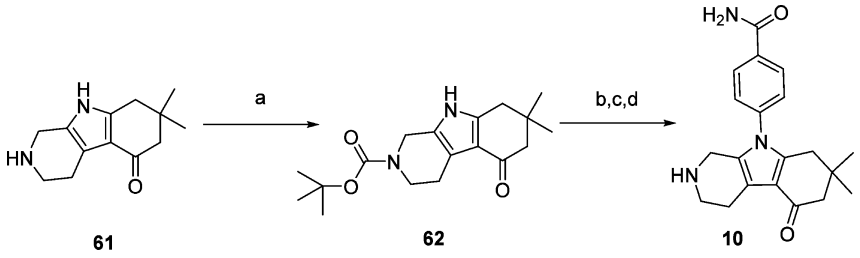

[a]Reagents and conditions: (a) $(BOC)_2O$, Et_3N, DCM, rt; (b) NaH, 4-fluorocyanobenzene, DMF, 150 °C; (c) TFA, DCM, rt; (d) NaOH, H_2O_2, EtOH, DMSO, rt.

Scheme 6. Synthesis of Octahydro-β-carboline Analogue 11[a]

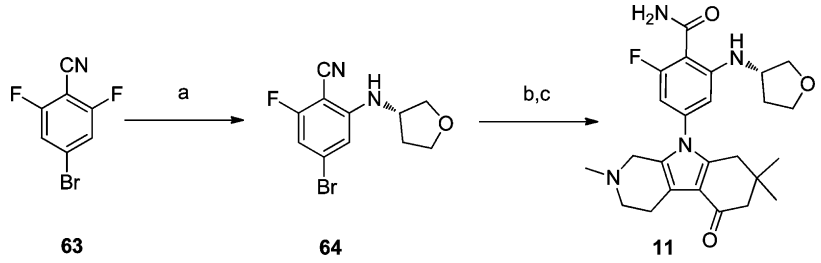

[a]Reagents and conditions: (a) (*S*)-tetrahydrofuran-3-amine, DIEA, DMSO, rt; (b) CuI, **59**, K_2CO_3, *N*,*N*′-dimethylethane-1,2-diamine, 1,4-dioxane, 100 °C; (c) NaOH, H_2O_2, EtOH, DMSO, rt.

Scheme 7. Synthesis of Octahydro-β-carboline Analogues 12−22[a]

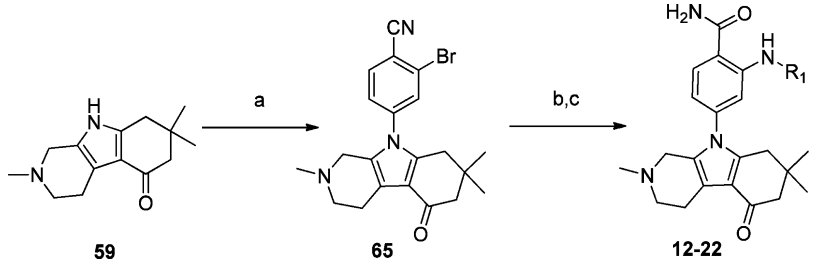

[a]Reagents and conditions: (a) NaH, 3-fluoro-5-cyanobromobenzene, DMF, 150 °C; (b) R_1NH_2, $Pd(OAc)_2$, dppf, NaOtBu, toluene, 110 °C; (c) NaOH, H_2O_2, EtOH, DMSO, rt.

Scheme 8. Synthesis of Benzolactam Analogue 23[a]

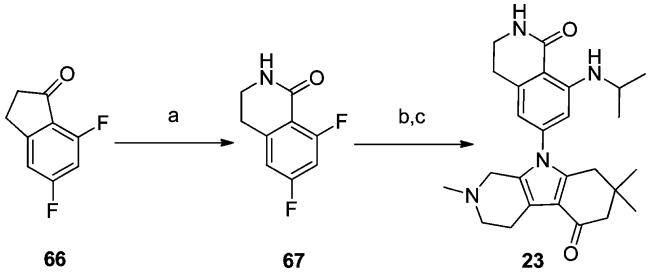

[a]Reagents and conditions: (a) methanesulfonic acid, NaN_3, DCM, 0 °C to rt; (b) isopropylamine, Et_3N, DMF, 180 °C; (c) NaH, **59**, DMF, 180 °C.

Scheme 9. Synthesis of Benzolactam Analogues 24−26[a]

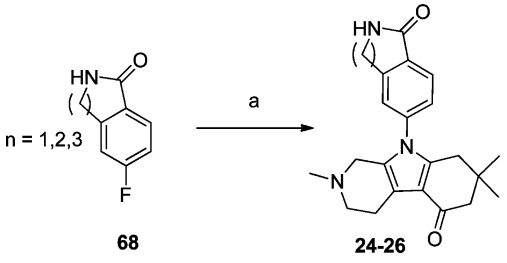

[a]Reagents and conditions: (a) NaH, **59**, DMF, 150 °C.

Determination of Huntingtin IC_{50} and CC_{50} Values in HD Patient Derived Fibroblasts. Compounds were tested in primary human fibroblasts for the ability to reduce the levels of Htt protein. HD patient derived fibroblasts were plated at 7.5×10^4 cells per well and dosed with varying concentrations of compound or DMSO for 48 h. Following incubation, cells were washed with PBS and lysed in Laemeli sample buffer with β-mercaptoethanol. Cell lysates were loaded onto a 4−12% Bis-tris gel, transferred onto a PVDF membrane. Following transfer, blots were washed with PBS containing 0.1% Tween 20, blocked in 5% nonfat milk PBST for 1 h, and probed with primary antibody directed against Htt protein and GAPDH as a loading control (mAb2166 Millipore 1:3000, Santa Cruz Biotechnology 25−778 1:5000). Following overnight incubation at 4 °C, blots were washed and probed with 2° HRP antibody. The blots were then developed using CL-Xposure clear blue X-ray film. GAPDH expression level is used as a loading control. For the determination of Htt IC_{50} values, the density of the Htt band at a specific compound

dx.doi.org/10.1021/jm500042s | J. Med. Chem. 2014, 57, 3382−3400

Scheme 10. Synthesis of Octahydro-β-carboline Analogue 27[a]

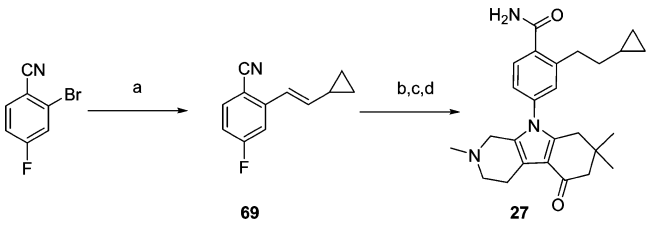

[a]Reagents and conditions: (a) 2-[(*E*)-2-cyclopropylvinyl]-4,4,5,5-tetramethyl-1,3,2-dioxaborolane, $PdCl_2$dppf, $tBuNH_2$, iPrOH, H_2O, 90 °C; (b) NaH, **59**, DMF, 170 °C; (c) 10% Pd on C, EtOAc, AcOH, 1 atm H_2, rt; (d) NaOH, H_2O_2, EtOH, DMSO, rt.

Scheme 11. Synthesis of Tetrahydroindolone−Benzolactam Derivatives 28 and 30−41[a]

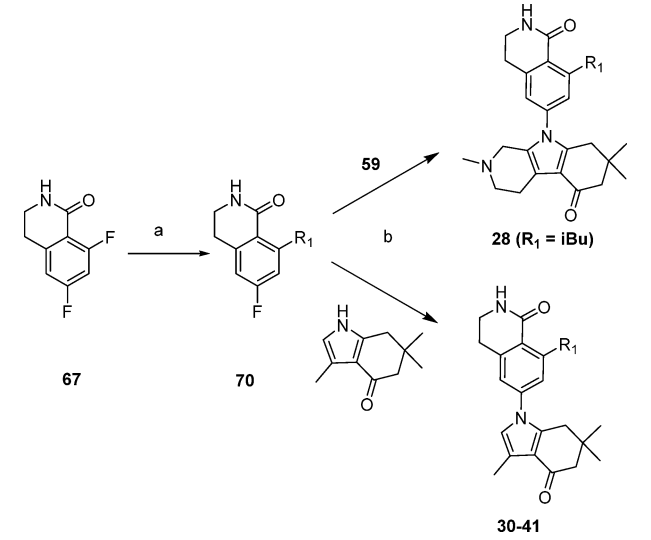

[a]Reagents and conditions: (a) R_1MgCl, THF, 110 °C; (b) NaH, **59** or 3,6,6-trimethyl-1,5,6,7-tetrahydro-4*H*-indol-4-one, DMF, 180 °C.

concentration was compared to a DMSO treated control cell sample present on each exposure. IC_{50} values are defined as the concentration of compound in which the density of the Htt protein band is 50% of the DMSO control. For determination of CC_{50} values, HD patient derived fibroblasts were plated at 7.5×10^4 cells per well and dosed with varying concentrations of compound or DMSO for 48 h. Following incubation, cell viability was determined using the Cell Titer Glo kit (Promega G7571) according to manufacturer's instructions. The signal in compound treated wells was normalized to solvent control wells and CC_{50} values were calculated. All reported IC_{50} and CC_{50} values are means of duplicate experiments.

Characterization of HSP90 Client Protein and HSP70 Levels in HD Patient Derived Fibroblasts. Compounds were tested in primary human fibroblasts for the ability to reduce the levels of HSP90 client proteins and increase the levels of HSP70. Human fibroblasts were plated at 7.5×10^4 cells per well and dosed with varying concentrations of compound or DMSO for 48 h. Following incubation, cells were washed with PBS and lysed in Laemeli sample buffer with β-mercaptoethanol. Cell lysates are loaded onto a 4−12% Bis-tris gel, transferred onto a PVDF membrane. Following transfer, blots are washed with PBS containing 0.1% Tween 20, blocked in 5% nonfat milk PBST for 1 h, and probed with primary antibody directed against HSP70, CDK4, AKT, and GAPDH as a loading control (no. 4876 Cell Signal 1:1000, SC-260 Santa Cruz Biotechnology 1:2000, no. 4619 Cell Signaling 1:1000, Santa Cruz Biotechnology 25-778 1:5000, respectively). Following overnight incubation at 4 °C, blots were washed and probed with 2° HRP antibody. The blot was then developed using CL-Xposure clear blue X-ray film. GAPDH expression level was used as a loading control.

Determination of Htt Protein Levels in Rat Brains. Male Sprague−Dawley rats weighing approximately 200 g were administered vehicle (0.5% methylcellulose, 0.5% sodium lauryl sulfate) or **31** (5 mg/kg) at a 5 mL/kg dose volume by oral gavage. At the appropriate time point following dosing, animals were briefly anesthetized in an isoflurane chamber (30 s) and then decapitated. Brains were dissected, and a horizontal corticostriatal slice (approximately 1 mm thick in diameter) was removed, flash frozen in liquid nitrogen, placed into Covaris S-series glass tubes, and stored at −80 °C. Cortical-striatal slices were homogenized in 1 mL of lysate buffer (1× PBS with 0.1% Tween 20, 0.1% SDS, protease inhibitors) using a Covaris E210 ultrasonicator (Covaris incorporated) to generate a brain lysate. Brain lysates were loaded onto a 4−12% Bis-tris gel, transferred onto a PVDF membrane. Following transfer, blots were washed with PBS containing 0.1% Tween 20, blocked in 5% nonfat milk PBST for 1 h, and probed with primary antibody directed against Htt protein and GAPDH as a loading control (mAb2166 Millipore 1:3000, Santa Cruz Biotechnology 25-778 1:5000). Following overnight incubation at 4 °C, blots were washed and probed with 2° HRP antibody. The blot was then developed using CL-Xposure clear blue X-ray film. GAPDH expression level was used as a loading control. The intensity of the Htt protein band in the compound treated animals was normalized to the corresponding GAPDH protein band. The normalized density of the Htt protein band in compound treated rats was then calculated as a percent of the normalized density of the Htt protein band in the vehicle controls.

General Procedure for the Preparation of 4-(Substituted-6,6-dimethyl-4-oxo-4,5,6,7-tetrahydro-1*H*-indol-1-yl)-benzamides (3−8). To a stirring solution of substituted-6,6-dimethyl-6,7-dihydro-1*H*-indol-4(5*H*)-one (0.15 mmol) in DMF (250 μL), under N_2, was added NaH (0.15 mmol, 60% in mineral oil). The solution was stirred at ambient temperature for 10 min, followed by the addition of 4-fluorobenzonitrile (0.46 mmol). The solution was heated at 150 °C for 5 min and then quenched with MeOH (100 μL) and DMSO (500 μL). The solution was filtered and purified by HPLC (10−90% ACN in water with HCl modifier) to obtain the nitrile intermediate **43**. The nitrile intermediate **43** was dissolved in EtOH (500 μL) and DMSO (50 μL). To this solution was added NaOH (1.0 M in water, 50 μL) and H_2O_2 (30% in water, 30 μL). The resulting mixture was stirred at rt for 1 h. The reaction was then evaporated to dryness under reduced pressure, diluted with DMSO (500 μL), filtered, and purified by preparative HPLC (10−90% ACN in water with HCl modifier) to obtain the desired product.

*4-(3,6,6-Trimethyl-4-oxo-4,5,6,7-tetrahydro-1H-indol-1-yl)-benzamide (**3**).* Yield 62%. ^{1}H NMR (500 MHz, DMSO-d_6) δ 8.11 (s, 1H), 8.00 (d, *J* = 8.4 Hz, 2H), 7.52−7.49 (m, 3H), 6.87 (s, 1H), 2.70 (s, 2H), 2.26 (s, 2H), 2.21 (s, 3H), 0.98 (s, 6H). ^{13}C NMR (126 MHz, DMSO-d_6) δ 194.47, 167.61, 142.26, 140.91, 133.23, 129.35, 124.44, 121.42, 119.13, 118.92, 52.40, 36.98, 35.62, 28.41, 11.79. HRMS (ESI): $[M + H]^+$ calcd for $C_{18}H_{20}N_2O_2$, 297.1598; found, 297.1599.

*4-(7,7-Dimethyl-9-oxo-6,7,8,9-tetrahydro-5H-pyrido[3,2-b]indol-5-yl)benzamide Hydrochloride (**4**).* Yield 55%. ^{1}H NMR (400 MHz, DMSO-d_6) δ 8.61 (d, *J* = 5.4 Hz, 1H), 8.17 (m, 4H), 7.73 (d, *J* = 8.3 Hz, 2H), 7.59 (m, 2H), 2.93 (s, 2H), 2.53 (s, 2H), 1.10 (s, 6H). HRMS (ESI): $[M + H]^+$ calcd for $C_{20}H_{19}N_3O_2$, 334.1550; found, 334.1551.

*4-(7,7-dimethyl-5-oxo-7,8-dihydro-5H-pyrido[3,4-b]indol-9(6H)-yl)benzamide Hydrochloride (**5**).* Yield 70%. ^{1}H NMR (400 MHz, DMSO-d_6) δ 9.61 (s, 1H), 8.82 (d, *J* = 8.0 Hz, 1H), 8.41 (d, *J* = 6.7 Hz, 1H), 8.30−8.10 (m, 3H), 7.98 (d, *J* = 8.7 Hz, 2H), 7.68 (s, 1H), 3.16 (s, 2H), 2.56 (s, 2H), 1.14 (s, 6H). HRMS (ESI): $[M + H]^+$ calcd for $C_{20}H_{19}N_3O_2$, 334.1550; found, 334.1552.

*4-(7,7-Dimethyl-5-oxo-7,8-dihydro-5H-pyrido[2,3-b]indol-9(6H)-yl)benzamide Hydrochloride (**6**).* Yield 74%. ^{1}H NMR (400 MHz, DMSO-d_6) δ 8.38 (dd, *J* = 7.7, 1.5 Hz, 1H), 8.27 (dd, *J* = 4.7, 1.5 Hz, 1H), 8.14 (s, 1H), 8.09 (d, *J* = 8.4 Hz, 2H), 7.67 (d, *J* = 8.4 Hz, 2H), 7.54 (s, 1H), 7.34 (dd, *J* = 7.8, 4.8 Hz, 1H), 2.86 (s, 2H), 2.45 (s, 2H),

dx.doi.org/10.1021/jm500042s | J. Med. Chem. 2014, 57, 3382−3400

1.08 (s, 6H). ^{13}C NMR (125 MHz, DMSO-d_6) δ 193.56, 167.78, 152.22, 149.36, 144.27, 137.42, 134.60, 129.04, 127.95, 119.73, 117.11, 110.36, 51.92, 36.54, 35.57, 28.41. HRMS (ESI): $[M + H]^+$ calcd for $C_{20}H_{19}N_3O_2$, 334.1550; found, 334.1552.

4-(2,2-Dimethyl-4-oxo-3,4,5,6,7,8-hexahydro-1H-carbazol-9(2H)-yl)benzamide (7). Yield 25%. ^{1}H NMR (400 MHz, DMSO-d_6) δ 8.08 (s, 1H), 8.01 (d, J = 8.5 Hz, 2H), 7.48 (s, 1H), 7.45 (d, J = 8.5 Hz, 2H), 2.72−2.67 (m, 2H), 2.53−2.49 (m, 2H), 2.36−2.30 (m, 2H), 2.22 (s, 2H), 1.73−1.69 (m, 4H), 0.99 (s, 6H). HRMS (ESI): $[M + H]^+$ calcd for $C_{21}H_{24}N_2O_2$, 337.1911; found, 337.1919.

4-(2,7,7-Trimethyl-5-oxo-3,4,5,6,7,8 hexahydro-1H-pyrido[3,4-b]-indol-9(2H)-yl)benzamide Hydrochloride (8). Yield 38%. ^{1}H NMR (400 MHz, CD_3OD) δ 8.10 (d, J = 8.6 Hz, 2H), 7.47 (d, J = 8.6 Hz, 2H), 4.29−4.22 (m, 2H), 3.6−3.724 (m, 1H), 3.57−3.39 (m, 1H), 3.25−3.10 (m, 3H), 2.99 (s, 3H), 2.83−2.13 (m, 5H), 1.10 (s, 3H), 1.03 (s, 3H). HRMS (ESI): $[M + H]^+$ calcd for $C_{21}H_{25}N_3O_2$, 352.2020; found, 352.2021.

4-(2,8,8-Trimethyl-6-*oxo*-2,3,4,5,6,7,8,9-octahydroazepino-[3,4-*b*]indol-10(1*H*)-yl)benzamide Hydrochloride (9). A solution of 2-(1,3-dioxolan-2-yl)-*N*-methyl-ethanamine **57** (530 mg, 4.0 mmol) and formaldehyde (300 μL of 37% w/w in water, 4.0 mmol) in AcOH was added slowly to 6,6-dimethyl-5,7-dihydro-1*H*-indol-4-one **55** (660 mg, 4.0 mmol) in AcOH (5 mL) at rt. The reaction was stirred for 5 h at 75 °C, diluted with water, and then extracted with Et_2O. The aqueous layer was basified with $NaHCO_3$ to pH 9 and extracted with DCM. The DCM layer was dried ($MgSO_4$), filtered, and concentrated under reduced pressure to yield the intermediate acetal (900 mg). The acetal was stirred in aq HCl (10 mL of 8 M, 80.0 mmol) for 25 min at 70 °C, diluted with water, and then basified with 1.0 M aq NaOH solution to pH 10. The mixture was extracted with DCM, and the combined organics were dried ($MgSO_4$), filtered, and concentrated under reduced pressure to yield the olefin intermediate (50 mg). The olefin intermediate was dissolved in EtOH (2 mL), and to this solution was added 10% Pd on C (50 mg, 0.46 mmol). The resulting mixture was stirred for 10 min under 1 atm of H_2. The mixture was filtered through a bed of Celite to give 2,8,8-trimethyl-2,3,4,5,7,8,9,10-octahydroazepino[3,4-*b*]indol-6(1*H*)-one **60** (49 mg, yield 3%) as a white solid. To a stirring solution of 2,8,8-trimethyl-2,3,4,5,7,8,9,10-octahydroazepino[3,4-*b*]indol-6(1*H*)-one **60** (37.0 mg, 0.15 mmol) in DMF (250 μL), under N_2, was added NaH (6.0 mg, 0.15 mmol, 60% in mineral oil). The solution was stirred at ambient temperature for 10 min, followed by the addition of 4-fluorobenzonitrile (56 mg, 0.46 mmol). The solution was heated at 100 °C for 8 h and then quenched with MeOH (100 μL) and DMSO (500 μL). The solution was filtered and purified by HPLC (10−90% ACN in water with HCl modifier) to obtain the nitrile intermediate. The nitrile intermediate was dissolved in EtOH (500 μL) and DMSO (50 μL). To this solution was added NaOH (1.0 M in water, 50 μL) and H_2O_2 (30% in water, 30 μL). The mixture was stirred at rt for 1 h. The reaction was evaporated to dryness under reduced pressure, diluted with DMSO (500 μL), filtered, and purified by preparative HPLC (10−90% ACN in water with HCl modifier) to obtain the desired product as a white solid (11 mg, 0.031 mmol, yield 21%). ^{1}H NMR (400 MHz, CD_3OD) δ 8.11 (d, J = 7.6 Hz, 2H), 7.49−7.38 (m, 2H), 4.36 (d, J = 15.2 Hz, 1H), 4.11 (d, J = 15.2 Hz, 1H), 3.70 (s, 1H), 3.64−3.33 (m, 4H), 3.23−3.02 (m, 1H), 2.79 (s, 3H), 2.47 (d, J = 2.9 Hz, 2H), 2.37 (s, 2H), 2.25−2.17 (m, 1H), 2.10−1.95 (m, 1H), 1.04 (s, 6H). HRMS (ESI): $[M + H]^+$ calcd for $C_{22}H_{27}N_3O_2$, 366.2176; found, 366.2172.

4-(7,7-Dimethyl-5-*oxo*-3,4,5,6,7,8-hexahydro-1*H*-pyrido[3,4-*b*]indol-9(2*H*)-yl)benzamide (10). A mixture of *tert*-butyl 7,7-dimethyl-5-*oxo*-1,3,4,6,8,9-hexahydropyrido[3,4-*b*]indole-2-carboxylate **62** (4.4 g, 13.9 mmol), 4-fluorobenzonitrile (2.1 g, 18.0 mmol), NaH (556 mg, 13.9 mmol, 60% in mineral oil), and DMF (44 mL) was heated at 150 °C for 5 min. The solution was directly purified via silica gel chromatography using 30% EtOAc in hexanes to obtain the nitrile intermediate. The nitrile intermediate (5 g, 11.9 mmol), TFA (27.2 g, 18.4 mL, 238 mmol), and DCM (15 mL) were stirred under N_2 at rt for 30 min. The solution was concentrated to dryness under reduced pressure and then dissolved in EtOH (15 mL) and DMSO (1 mL). To this solution was added NaOH (5.0 M in water, 3 mL) and H_2O_2 (30% in water, 3 mL). The solution was stirred at rt for 1 h. The reaction was acidified to pH 4 using AcOH and purified via silica gel chromatography using 10% MeOH in DCM to obtain the desired compound as a white solid (3.5g, 10.4 mmol, yield 75%). ^{1}H NMR (400 MHz, D_2O) δ 7.92 (d, J = 8.6 Hz, 2H), 7.41 (d, J = 8.6 Hz, 2H), 4.05 (s, 2H), 3.45 (t, J = 6.1 Hz, 2H), 3.04 (s, 2H), 2.56 (s, 2H), 2.37 (s, 2H), 1.98 (s, 1H), 0.96 (s, 6H). HRMS (ESI): $[M + H]^+$ calcd for $C_{20}H_{23}N_3O_2$, 338.1863; found, 338.1868.

2-Fluoro-6-(((*S*)-tetrahydrofuran-3yl)amino)-4-(2,7,7-trimethyl-5-*oxo*-decahydro-1*H*-pyrido[3,4-*b*] indol-9(9a*H*)-yl)-benzamide (11). To a solution of (*S*)-4-bromo-2-fluoro-6-((tetrahydrofuran-3-yl) amino)benzonitrile **64** (625 mg, 2.19 mmol) and 2,7,7-trimethyl-1,3,4,6,8,9-hexahydropyrido[3,4-*b*]indol-5-one **59** (509 mg, 2.19 mmol) in 1,4-dioxane (7.5 mL), under N_2 in a microwave vessel, was added K_2CO_3 (1.5 g, 11.0 mmol). CuI (626 mg, 3.28 mmol) and *N*,*N*′-dimethylethane-1,2-diamine (289 mg, 359 μL, 3.28 mmol) were added. The microwave vessel was sealed with a septa cap and heated at 100 °C in an oil bath for 19 h. The mixture was filtered through a bed of Celite followed by EtOAc (300 mL). The filtrate was evaporated to dryness under reduced pressure. The residue was purified by silica gel chromatography using 10% MeOH in DCM to obtain the nitrile intermediate. The nitrile intermediate was dissolved in EtOH (1.5 mL) and DMSO (300 μL). To this solution was added NaOH (1.0 M in water, 300 μL) and H_2O_2 (30% in water, 300 μL). The solution was stirred at rt for 1 h. The reaction was acidified to pH 4 using AcOH and purified by silica gel chromatography using 10% MeOH in DCM to obtain the desired compound as a white solid (50 mg, 0.11 mmol, yield 5%). ^{1}H NMR (400 MHz, DMSO-d_6) δ 7.79 (s, 2H), 7.31 (d, J = 6.9 Hz, 1H), 6.55 (dd, J = 11.2, 1.8 Hz, 1H), 6.44 (s, 1H), 4.15 (s, 1H), 3.93−3.77 (m, 2H), 3.75−3.71 (m, 1H), 3.56−3.53 (m, 1H), 3.23 (s, 2H), 2.70 (s, 2H), 2.64−2.55 (m, 4H), 2.30 (s, 3H), 2.23 (s, 3H), 1.79−1.66 (m, 1H), 1.00 (s, 6H). HRMS (ESI): $[M + H]^+$ calcd for $C_{25}H_{31}FN_4O_3$, 455.2453; found, 455.2456.

General Procedure for the Preparation of 2-(Aminoalkyl)-4-(2,7,7-trimethyl-5-*oxo*-3,4,5,6,7,8-hexahydro-1*H*-pyrido[3,4-*b*]-indol-9(2*H*)-yl)benzamides (12−22). A microwave vessel was loaded with 2-bromo-4-(2,7,7-trimethyl-5-*oxo*-3,4,6,8-tetrahydro-1*H*-pyrido[3,4-*b*]indol-9-yl)benzonitrile **65** (0.73 mmol), amine (0.73 mmol), sodium *tert*-butoxide (1.45 mmol), $Pd(OAc)_2$ (0.072 mmol), and dppf (0.072 mmol). The vessel was purged with N_2, and toluene (6 mL) was added via syringe. The mixture was heated at 110 °C for 20 min via microwave irradiation. The mixture was filtered through a bed of silica gel (1 g) using 10% MeOH in DCM (50 mL). The filtrate was then evaporated to dryness under reduced pressure to obtain the desired nitrile intermediate. The nitrile intermediate was dissolved in EtOH (1.5 mL) and DMSO (300 μL). To this solution was added NaOH (1.0 M in water, 300 μL) and H_2O_2 (30% in water, 300 μL). The solution was stirred at rt for 1 h. The reaction was acidified to pH 4 using AcOH and purified via silica gel chromatography using 10% MeOH in DCM or purified by preparative HPLC (10−90% ACN in water with HCl modifier) to obtain the desired compound.

(S)-2-((Tetrahydrofuran-3-yl)amino)-4-(2,7,7-trimethyl-5-oxo-3,4,5,6,7,8-hexahydro-1H-pyrido[3,4-b]indol-9(2H)-yl)benzamide (12). Yield 68%. ^{1}H NMR (400 MHz, DMSO-d_6) δ 8.49 (d, J = 6.8 Hz, 1H), 7.96 (s, 1H), 7.74 (d, J = 8.3 Hz, 1H), 7.31 (s, 1H), 6.57 (d, J = 1.9 Hz, 1H), 6.52 (dd, J = 8.2, 1.9 Hz, 1H), 4.22−4.01 (m, 1H), 3.93−3.68 (m, 3H), 3.54 (dd, J = 8.9, 2.9 Hz, 1H), 3.20 (s,1H), 3.17 (s, 2H), 2.79−2.68 (m, 2H), 2.63−2.54 (m, 3H), 2.29 (s, 2H), 2.26−2.21 (m, 2H), 1.91 (s, 1H), 1.77−1.68 (m, 1H), 1.00 (s, 6H). HRMS (ESI): $[M + H]^+$ calcd for $C_{25}H_{32}N_4O_3$, 437.2547; found, 437.2547.

2-(Cyclopentylamino)-4-(2,7,7-trimethyl-5-oxo-3,4,5,6,7,8-hexahydro-1H-pyrido[3,4-b]indol-9(2H)-yl)benzamide Hydrochloride (13). Yield 73%. ^{1}H NMR (400 MHz, DMSO-d_6) δ 11.21 (s, 1H), 8.01 (s, 1H), 7.80 (d, J = 8.3 Hz, 1H), 7.31 (s, 1H), 6.55 (d, J = 1.9 Hz, 1H), 6.48 (dd, J = 8.3, 2.0 Hz, 1H), 4.20−4.18 (m, 2H), 3.93−3.76 (m, 1H), 3.60−3.54 (m, 1H), 3.35−3.29 (m, 1H), 3.10−3.00 (m, 2H), 2.83 (d, J = 4.7 Hz, 3H), 2.76 (d, J = 16.5 Hz, 1H), 2.35 (d, J = 15.9 Hz, 1H), 2.21 (d, J = 15.9 Hz, 1H), 2.09−1.96 (m, 2H), 1.77−1.51 (m, 4H), 1.51−1.35 (m, 2H), 1.51 (s, 3H), 0.97 (s, 3H). HRMS (ESI): $[M + H]^+$ calcd for $C_{26}H_{34}N_4O_2$, 435.2755; found, 435.2756.

*2-((Cyclopropylmethyl)amino)-4-(2,7,7-trimethyl-5-oxo-3,4,5,6,7,8-hexahydro-1H-pyrido[3,4-b]indol-9(2H)-yl)benzamide (**14**).* Yield 77%. ^{1}H NMR (400 MHz, DMSO-d_6) δ 8.35 (t, J = 5.1 Hz, 1H), 7.93 (s, 1H), 7.72 (d, J = 8.3 Hz, 1H), 7.27 (s, 1H), 6.50 (d, J = 2.0 Hz, 1H), 6.46 (dd, J = 8.2, 2.0 Hz, 1H), 3.18 (d, J = 5.5 Hz, 3H), 3.00 (dd, J = 6.5, 5.4 Hz, 2H), 2.73−2.68 (m, 2H), 2.59−2.51 (m, 3H), 2.28 (s, 3H), 2.22 (s, 2H), 1.13−1.02 (m, 1H), 0.99 (s, 6H), 0.57−0.42 (m, 2H), 0.27−0.14 (m, 2H). HRMS (ESI): [M + H]$^+$ calcd for $C_{25}H_{32}N_4O_2$, 421.2598; found, 421.2599.

*2-((2-Methoxyethyl)amino)-4-(2,7,7-trimethyl-5-oxo-3,4,5,6,7,8-hexahydro-1H-pyrido[3,4-b]indol-9(2H)-yl)benzamide Hydrochloride (**15**).* Yield 62%. ^{1}H NMR (400 MHz, DMSO-d_6) δ 11.12 (s, 1H), 7.98 (s, 1H), 7.79 (d, J = 8.3 Hz, 1H), 7.29 (s, 1H), 6.58 (d, J = 2.0 Hz, 1H), 6.49 (dd, J = 8.2, 2.0 Hz, 1H), 4.20−4.15 (m, 2H), 3.60−3.53 (m, 3H), 3.38−3.22 (m, 6H), 3.09−3.01 (m, 2H), 2.83 (d, J = 4.7 Hz, 3H), 2.76 (d, J = 16.6 Hz, 1H), 2.35 (d, J = 15.9 Hz, 2H), 2.20 (d, J = 15.9 Hz, 2H), 1.05 (s, 3H), 0.97 (s, 3H). HRMS (ESI): [M + H]$^+$ calcd for $C_{24}H_{32}N_4O_3$, 425.2547; found, 425.2548.

*2-((Tetrahydro-2H-thiopyran-4-yl)amino)-4-(2,7,7-trimethyl-5-oxo-3,4,5,6,7,8-hexahydro-1H-pyrido[3,4-b]indol-9(2H)-yl)-benzamide Hydrochloride (**16**).* Yield 72%. ^{1}H NMR (400 MHz, DMSO-d_6) δ 10.40 (s, 1H), 7.99 (s, 1H), 7.79 (d, J = 8.4 Hz, 1H), 7.35 (s, 1H), 6.61 (d, J = 1.9 Hz, 1H), 6.47 (dd, J = 8.3, 1.9 Hz, 1H), 3.55−3.40 (m, 2H), 3.29−3.25 (m, 1H), 3.05−3.02 (m, 2H), 2.89−2.85 (m, 3H), 2.83−2.61 (m, 6H), 2.25−2.09 (m, 6H), 1.60−1.48 (m, 2H), 1.05 (s, 3H), 0.96 (s, 3H). HRMS (ESI): [M + H]$^+$ calcd for $C_{26}H_{34}N_4O_2S$, 467.2476; found, 467.2478.

*2-(Propylamino)-4-(2,7,7-trimethyl-5-oxo-3,4,5,6,7,8-hexahydro-1H-pyrido[3,4-b]indol-9(2H)-yl)benzamide Hydrochloride (**17**).* Yield 81%. ^{1}H NMR (400 MHz, DMSO-d_6) δ 11.04 (s, 1H), 8.05 (d, J = 39.9 Hz, 1H), 7.80 (d, J = 8.2 Hz, 1H), 7.32 (s, 1H), 6.53 (s, 1H), 6.48 (d, J = 8.2 Hz, 1H), 4.22−4.18 (m, 2H), 3.61−3.56 (m 1H), 3.33−3.29 (m,1H), 3.55−3.00 (m, 2H), 3.04 (s, 2H), 2.84 (d, J = 4.4 Hz, 3H), 2.76 (d, J = 16.5 Hz, 1H), 2.35 (d, J = 16.0 Hz, 1H), 2.23 (d, J = 16.0 Hz, 1H), 1.60−1.50 (m, 2H), 1.17−0.89 (m, 9H). HRMS (ESI): [M + H]$^+$ calcd for $C_{24}H_{32}N_4O_2$, 409.2598; found, 409.2597.

*2-(Cyclopropylamino)-4-(2,7,7-trimethyl-5-oxo-3,4,5,6,7,8-hexahydro-1H-pyrido[3,4-b]indol-9(2H)-yl)benzamide Hydrochloride (**18**).* Yield 71%. ^{1}H NMR (400 MHz, DMSO-d_6) δ 11.15 (s, 1H), 8.02 (s, 1H), 7.81 (d, J = 8.3 Hz, 1H), 7.35 (s, 1H), 6.88 (d, J = 2.1 Hz, 1H), 6.57 (dd, J = 8.3, 2.1 Hz, 1H), 4.24−4.20 (m, 3H), 3.62−3.55 (m, 1H), 3.39−3.24 (m, 1H), 3.17 (s, 1H), 3.09−3.05 (m, 2H), 2.87−2.75 (m, 4H), 2.49−2.42 (m, 1H), 2.38 (dd, J = 16.0 Hz, 1H), 2.28 (dd, J = 16.0 Hz, 1H), 1.05 (s, 3H), 0.98 (s, 3H), 0.91−0.70 (m, 2H), 0.60−0.30 (m, 2H). HRMS (ESI): [M + H]$^+$ calcd for $C_{24}H_{30}N_4O_2$, 407.2442; found, 407.2442.

*2-((2,2-Difluoroethyl)amino)-4-(2,7,7-trimethyl-5-oxo-3,4,5,6,7,8-hexahydro-1H-pyrido[3,4-b]indol-9(2H)-yl)benzamide Hydrochloride (**19**).* Yield 58%. ^{1}H NMR (400 MHz, DMSO-d_6) δ 10.83 (s, 1H), 8.65 (s, 1H), 8.06 (s, 1H), 7.82 (d, J = 8.3 Hz, 1H), 7.43 (s, 1H), 6.77 (s, 1H), 6.69−6.52 (m, 1H), 6.48−5.96 (m, 1H), 3.73 (t, J = 15.8 Hz, 2H), 3.62−3.57 (m, 1H), 3.35−3.18 (m, 1H), 3.09−3.01 (m, 2H), 2.89−2.84 (m, 3H), 2.77 (d, J = 16.5 Hz, 1H), 2.35 (d, J = 15.9 Hz, 2H), 2.23 (d, J = 15.9 Hz, 2H), 1.05 (s 3H), 0.97 (s, 3H). HRMS (ESI): [M + H]$^+$ calcd for $C_{23}H_{28}F_2N_4O_2$, 431.2253; found, 431.2252.

*2-(((3-Methyloxetan-3-yl)methyl)amino)-4-(2,7,7-trimethyl-5-oxo-3,4,5,6,7,8-hexahydro-1H pyrido[3,4-b]indol-9(2H)-yl)-benzamide Hydrochloride (**20**).* Yield 77%. ^{1}H NMR (400 MHz, DMSO-d_6) δ 10.79 (s, 1H), 8.06 (d, J = 36.2 Hz, 1H), 7.80 (d, J = 8.3 Hz, 1H), 7.33 (s, 1H), 6.66 (d, J = 1.9 Hz, 1H), 6.46 (dd, J = 8.3, 1.9 Hz, 1H), 4.22−4.15 (m, 2H), 3.62−3.57 (m, 3H), 3.45−3.22 (m, 3H), 3.15−3.09 (m, 2H), 3.06−3.01 (m, 2H), 2.85 (d, J = 4.7 Hz, 3H), 2.74 (d, J = 16.5 Hz, 1H), 2.35 (d, J = 15.9 Hz, 1H), 2.22 (d, J = 15.9 Hz, 1H), 1.05 (s, 3H), 1.01−0.97 (m, 6H). HRMS (ESI): [M + H]$^+$ calcd for $C_{26}H_{34}N_4O_3$, 451.2704; found, 451.2687.

*2-(Isopropylamino)-4-(2,7,7-trimethyl-5-oxo-3,4,5,6,7,8-hexahydro-1H-pyrido[3,4-b]indol-9(2H)-yl)benzamide Hydrochloride (**21**).* Yield 64%. ^{1}H NMR (400 MHz, DMSO-d_6) δ 10.93 (s, 1H), 7.98 (s, 1H), 7.79 (d, J = 8.3 Hz, 1H), 7.32 (s, 1H), 6.54 (d, J = 1.9 Hz, 1H), 6.46 (dd, J = 8.3, 2.0 Hz, 1H), 4.19 (d, J = 4.9 Hz, 2H), 3.81−3.64 (m, 1H), 3.62−3.58 (m 1H), 3.39−3.21 (m, 1H), 3.17 (s, 1H), 3.09−3.01 (m, 2H), 2.84 (d, J = 4.7 Hz, 3H), 2.76 (d, J = 16.5 Hz, 1H), 2.39−2.16 (m, 2H), 1.28−1.12 (m, 6H), 1.05 (s, 3H), 0.97 (s, 3H). HRMS (ESI): [M + H]$^+$ calcd for $C_{24}H_{32}N_4O_2$, 409.2598; found, 409.2600.

*2-(Neopentylamino)-4-(2,7,7-trimethyl-5-oxo-3,4,5,6,7,8-hexahydro-1H-pyrido[3,4-b]indol-9(2H)-yl)benzamide Hydrochloride (**22**).* Yield 89%. ^{1}H NMR (400 MHz, DMSO-d_6) δ 11.00 (s, 1H), 8.01 (s, 1H), 7.81 (d, J = 8.3 Hz, 1H), 7.31 (s, 1H), 6.58 (d, J = 2.0 Hz, 1H), 6.44 (dd, J = 8.3, 2.0 Hz, 1H), 4.17 (d, J = 4.6 Hz, 2H), 3.62−3.58 (m, 1H), 3.41−3.18 (m, 1H), 3.06−3.01 (m, 2H), 2.93 (d, J = 5.7 Hz, 2H), 2.83 (d, J = 4.7 Hz, 3H), 2.73 (d, J = 16.5 Hz, 1H), 2.42 (d, J = 5.9 Hz, 2H), 2.22 (d, J = 5.9 Hz, 2H), 1.05 (s, 3H), 0.99−0.96 (m, 12H). HRMS (ESI): [M + H]$^+$ calcd for $C_{26}H_{36}N_4O_2$, 437.2911; found, 437.2912.

9-(8-(Isopropylamino)-1-*oxo*-1,2,3,4-tetrahydroisoquinolin-6-yl)-2,7,7-trimethyl-3,4,6,7,8,9-hexahydro-1*H*-pyrido[3,4-*b*]-indol-5(2*H*)-one (23). A microwave vessel was loaded with 6,8-difluoro-3,4-dihydro-2*H*-isoquinolin-1-one **67** (250 mg, 1.37 mmol), Et_3N (414 mg, 570 μL, 4.10 mmol), and DMF (250 μL). To this solution was added propan-2-amine (403 mg, 586 μL, 6.83 mmol). The mixture was heated at 180 °C for 10 min via microwave irradiation. The residue was purified via silica gel chromatography using 30% EtOAc in hexanes to obtain the intermediate aniline (239 mg). The aniline was added to a preformed solution of 2,7,7-trimethyl-1,3,4,6,8,9-hexahydropyrido[3,4-*b*]indol-5-one **59** (250 mg, 1.08 mmol), NaH (86 mg, 2.15 mmol, 60% in mineral oil), and DMF (1.2 mL). The solution was heated via microwave irradiation at 180 °C for 10 min. The reaction was quenched with MeOH (300 μL), neutralized with AcOH, and purified via silica gel chromatography using 3% MeOH in DCM to obtain a white solid (152 mg, 0.35 mmol, yield 26%). ^{1}H NMR (400 MHz, DMSO-d_6) δ 8.80 (d, J = 7.6 Hz, 1H), 7.83 (s, 1H), 6.40 (d, J = 1.7 Hz, 1H), 6.33 (d, J = 1.6 Hz, 1H), 3.71−3.64 (m, 1H), 3.21 (s, 2H), 3.17 (s, 2H), 2.86−2.80 (m, 2H), 2.73−2.65 (m, 2H), 2.63−2.57 (m, 4H), 2.29 (s, 3H), 2.23 (s, 2H), 1.16 (d, J = 6.2 Hz, 6H), 1.00 (s, 6H). HRMS (ESI): [M + H]$^+$ calcd for $C_{26}H_{34}N_4O_2$, 435.2755; found, 435.2755.

General Procedure for the Preparation of 4-(2,7,7-Trimethyl-5-*oxo*-3,4,5,6,7,8-hexahydro-1*H*-pyrido[3,4-*b*]indol-9(2*H*)-yl)benzolactams (24−26). A microwave vessel was loaded with 2,7,7-trimethyl-1,3,4,6,8,9-hexahydropyrido[3,4-*b*]indol-5-one **59** (0.22 mmol) and DMF (1 mL). NaH (0.32 mmol, 60% in mineral oil) was added under N_2, and the solution was stirred for 10 min. The fluorobenzolactam **68** (0.32 mmol) was added, and the solution was heated via microwave irradiation at 150 °C for 10 min. The reaction was diluted with DMSO (500 μL), filtered, and purified by HPLC (10−90% ACN in water with HCl modifier) to obtain the desired product.

*2,7,7-Trimethyl-9-(1-oxo-isoindolin-5-yl)-3,4,6,7,8,9-hexahydro-1H-pyrido[3,4-b]indol-5(2H)-one Hydrochloride (**24**).* Yield 62%. ^{1}H NMR (400 MHz, DMSO-d_6) δ 10.81 (s, 1H), 8.78 (s, 1H), 7.87 (d, J = 8.0 Hz, 1H), 7.64 (s, 1H), 7.47 (dd, J = 8.0, 1.7 Hz, 1H), 4.48 (s, 2H), 4.20−4.15 (m, 2H), 3.65−3.58 (m, 1H), 3.32−3.28 (m, 1H), 3.07−3.03 (m, 2H), 2.85−2.81 (m, 3H), 2.72 (d, J = 16.6 Hz, 1H), 2.35 (d, J = 16.0 Hz, 1H), 2.25 (d, J = 16.0 Hz, 1H), 1.05 (s, 3H), 0.98 (s, 3H). HRMS (ESI): [M + H]$^+$ calcd for $C_{22}H_{25}N_3O_2$, 364.2020; found, 364.2021.

*2,7,7-Trimethyl-9-(1-oxo-1,2,3,4-tetrahydroisoquinolin-6-yl)-3,4,6,7,8,9-hexahydro-1H-pyrido[3,4-b]indol-5(2H)-one Hydrochloride (**25**).* Yield 82%. ^{1}H NMR (400 MHz, DMSO-d_6) δ 10.30 (s, 1H), 8.11 (s, 1H), 8.04 (d, J = 8.1 Hz, 1H), 7.40−7.29 (m, 2H), 4.21 (s, 2H), 3.69−3.62 (m, 1H), 3.35−3.22 (m, 4H), 3.08−2.98 (m, 4H), 2.89−2.86 (m, 3H), 2.76−2.68 (m, 1H), 2.35 (d, J = 15.6 Hz, 1H), 2.25 (d, J = 15.6 Hz, 1H), 1.06 (s, 3H), 0.98 (s, 3H). ^{13}C NMR (100 MHz, DMSO-d_6) δ 193.07, 163.45, 143.42, 141.41, 137.54, 129.41, 128.75, 125.03, 124.47, 121.57, 116.44, 112.70, 51.73, 50.68, 48.52, 41.60, 35.63, 35.18, 28.50, 27.54, 27.41, 19.57. HRMS (ESI): [M + H]$^+$ calcd for $C_{23}H_{27}N_3O_2$, 378.2176; found, 378.2178.

*2,7,7-Trimethyl-9-(1-oxo-2,3,4,5-tetrahydro-1H-benzo[c]azepin-7-yl)-3,4,6,7,8,9-hexahydro-1H-pyrido[3,4-b]indol-5(2H)-one Hydrochloride (**26**).* Yield 67%. ^{1}H NMR (400 MHz, DMSO-d_6) δ 9.99 (s, 1H), 8.22 (t, J = 5.9 Hz, 1H), 7.70 (d, J = 8.0 Hz, 1H), 7.34 (d, J = 8.1 Hz, 1H), 4.25−4.20 (m, 2H), 3.64−3.60 (m, 1H), 3.10−2.93 (m, 4H),

2.89−2.87 (m, 3H), 2.85−2.81 (m, 2H), 2.73 (d, J = 16.5 Hz, 1H), 2.46−2.42 (m, 1H), 2.35 (d, J = 15.9 Hz, 1H), 2.25 (d, J = 15.9 Hz, 1H), 2.04−1.77 (m, 2H), 1.05 (s, 3H), 0.98 (s, 3H). HRMS (ESI): $[M + H]^+$ calcd for $C_{24}H_{29}N_3O_2$, 392.2333; found, 392.2334.

2-(2-Cyclopropylethyl)-4-(2,7,7-trimethyl-5-*oxo*-3,4,5,6,7,8-hexahydro-1*H*-pyrido[3,4-*b*]indol-9(2*H*)-yl)benzamide Hydrochloride (27). A mixture of (*E*)-2-(2-cyclopropylvinyl)-4-fluorobenzonitrile **69** (63 mg, 0.34 mmol) and 2,7,7-trimethyl-1,3,4,6,8,9-hexahydropyrido[3,4-*b*]indol-5-one **59** (78 mg, 0.34 mmol), DMF (1.5 mL), and NaH (12 mg, 0.50 mmol, 60% in mineral oil) was heated at 170 °C via microwave irradiation for 1 h. The mixture was partitioned between EtOAc and water. The organic phase was dried, filtered, and concentrated under reduced pressure. The residue was purified by silica gel chromatography using 0−30% MeOH in DCM to obtain the intermediate olefin. The olefin product was added to EtOAc (945 μL), AcOH (315 μL), and 10% Pd on C (35 mg, 0.33 mmol) and stirred under 1 atm of H_2 for 30 min. The mixture was filtered, and the filtrate was concentrated under reduced pressure. The residue was purified by silica gel chromatography using 0−30% MeOH in DCM to obtain the intermediate nitrile. The nitrile intermediate was dissolved in EtOH (378 μL) and DMSO (38 μL). To this solution was added NaOH (1.0 M in water, 37 μL) and H_2O_2 (30% in water, 10 μL). The solution was stirred at rt for 1 h. The reaction was acidified to pH 4 using AcOH and purified by preparative HPLC (10−90% ACN in water with HCl modifier) to obtain a white solid (12 mg, 0.03 mmol, yield 9%). ^{1}H NMR (400 MHz, $CDCl_3$) δ 7.48 (d, J = 8.0 Hz, 1H), 7.06 (d, J = 2.0 Hz, 1H), 7.01 (dd, J = 8.0, 2.1 Hz, 1H), 5.81−5.70 (bs, 2H), 3.19 (s, 2H), 2.97−2.85 (m, 4H), 2.65−2.60 (m, 2H), 2.37 (s, 2H), 2.34 (s, 3H), 2.26 (s, 2H), 1.50 (dd, J = 15.1, 7.2 Hz, 2H), 0.99 (s, 6H), 0.70−0.62 (m, 1H), 0.45−0.27 (m, 2H), 0.06−0.13 (m, 2H). HRMS (ESI): $[M + H]^+$ calcd for $C_{26}H_{33}N_3O_2$, 420.2646; found, 420.2648.

9-(8-Isobutyl-1-*oxo*-1,2,3,4-tetrahydroisoquinolin-6-yl)-2,7,7-trimethyl-3,4,6,7,8,9-hexahydro-1*H*-pyrido[3,4-*b*]indol-5(2*H*)-one (28). A microwave vessel was loaded with 2,7,7-trimethyl-1,3,4,6,8,9-hexahydropyrido[3,4-*b*]indol-5-one **59** (250 mg, 1.076 mmol) and DMF (1.3 mL). NaH (86 mg, 2.15 mmol, 60% in mineral oil) was added under N_2, and the solution was stirred for 15 min. To this solution was added 6-fluoro-8-isobutyl-3,4-dihydro-2*H*-isoquinolin-1-one (238 mg, 1.08 mmol), and the solution was heated via microwave at 180 °C for 10 min. The reaction was quenched with MeOH (300 μL), neutralized with AcOH, and purified via silica gel chromatography using 3% MeOH in DCM to obtain a white solid (156 mg, 33.6 mmol, yield 33%). ^{1}H NMR (400 MHz, DMSO-d_6) δ δ 7.97 (s, 1H), 7.20 (d, J = 2.0 Hz, 1H), 7.05 (d, J = 2.1 Hz, 1H), 3.19 (bs, 1H), 3.17 (s, 3H), 3.02 (d, J = 6.9 Hz, 2H), 2.95−2.89 (m, 2H), 2.74−2.68 (m, 2H), 2.62−2.55 (m, 3H), 2.29−2.56 (m, 2H), 2.23 (bs, 1H), 1.96−1.82 (m, 2H), 0.99 (s, 6H), 0.85 (d, J = 6.6 Hz, 6H). HRMS (ESI): $[M + H]^+$ calcd for $C_{27}H_{35}N_3O_2$, 434.2802; found, 434.2804.

(*S*)-4-(2,2-Dimethyl-4-*oxo*-3,4,5,6,7,8-hexahydro-1*H*-carbazol-9(2*H*)-yl)-2-((tetrahydrofuran-3 yl)amino)benzamide Hydrochloride (29). A microwave vessel was loaded with 2-bromo-4-(7,7-dimethyl-5-*oxo*-1,2,3,4,6,8-hexahydrocarbazol-9-yl)benzonitrile (30 mg, 0.08 mmol), (*S*)-tetrahydrofuran-3-amine (9.3 mg, 0.08 mmol), $Pd(OAc)_2$ (1.7 mg, 0.008 mmol), DPPF (4.1 mg, 0.008 mmol), sodium *tert*-butoxide (14.5 mg, 0.15 mmol), and toluene (600 μL). The vessel was purged with N_2, and the mixture was heated via a preheated oil bath at 150 °C for 20 min. The mixture was directly passed through a short plug of silica gel (1 g) using EtOAc (5 mL). The filtrate was concentrated under reduced pressure to obtain the nitrile intermediate. The nitrile intermediate was dissolved in EtOH (400 μL) and DMSO (100 μL). To this solution was added NaOH (1.0 M in water, 100 μL) and H_2O_2 (30% in water, 30 μL). The solution was stirred at rt for 1 h. The reaction was acidified to pH 4 using AcOH, diluted with DMSO (500 μL), filtered, and purified by HPLC (10−90% ACN in water with HCl modifier) to obtain a white solid (15 mg, 0.036 mmol, yield 45%). ^{1}H NMR (400 MHz, DMSO-d_6) δ 8.49 (d, J = 6.7 Hz, 1H), 7.95 (bs, 1H), 7.74 (d, J = 8.3 Hz, 1H), 7.29 (bs, 1H), 6.57 (s, 1H), 6.51 (dd, J = 8.3, 1.9 Hz, 1H), 4.22−4.06 (m, 1H), 3.90−3.70 (m, 3H), 3.54 (dd, J = 8.9, 3.0 Hz, 1H), 2.66 (s, 2H), 2.56−2.53 (m, 2H), 2.36 (s, 2H), 2.31−2.13 (m, 3H), 1.88−1.60 (m, 5H), 1.00 (s, 6H). HRMS (ESI): $[M + H]^+$ calcd for $C_{25}H_{31}N_3O_3$, 422.2438; found, 422.2440.

General Procedure for the Preparation of 8-Substituted-6-(3,6,6-trimethyl-4-*oxo*-4,5,6,7-tetrahydro-1*H*-indol-1-yl)-3,4-dihydroisoquinolin-1(2*H*)-one (30−41). A microwave vessel was loaded with 6,8-difluoro-3,4-dihydro-2*H*-isoquinolin-1-one **67** (0.44 mmol). To this was added a solution of the Grignard reagent (1.75 mmol). The mixture was heated at 110 °C via microwave irradiation for 5 min. The reaction was quenched with 10% MeOH in DCM (1 mL) and evaporated to dryness under reduced pressure. The residue was passed through a short plug of silica gel (1 g) using 10% MeOH in DCM (8 mL). The filtrate was evaporated to dryness under reduced pressure, and the residue was added to a preformed solution of 3,6,6-trimethyl-6,7-dihydro-1*H*-indol-4(5*H*)-one (0.22 mmol), NaH (0.44 mmol, 60% in mineral oil), and DMF (800 μL) that had been stirred at rt for 15 min. The reaction was then heated via microwave irradiation at 180 °C for 15 min. The reaction was diluted with DMSO (500 μL), filtered, and purified by preparative HPLC (10−99% ACN in water with HCl modifier) to obtain the desired product.

*8-Isobutyl-6-(3,6,6-trimethyl-4-oxo-4,5,6,7-tetrahydro-1H-indol-1-yl)-3,4-dihydroisoquinolin-1(2H)-one (**30**).* Yield 52%. ^{1}H NMR (500 MHz, DMSO-d_6) δ 7.93 (s, 1H), 7.23 (s, 1H), 7.10 (s, 1H), 6.84 (s, 1H), 3.28 (s, 2H), 3.02 (d, J = 6.8 Hz, 2H), 2.90 (t, J = 5.9 Hz, 2H), 2.71 (s, 2H), 2.25 (s, 2H), 2.21 (s, 3H), 1.86 (dt, J = 13.2, 6.4 Hz, 1H), 0.98 (s, 6H), 0.85 (d, J = 6.6 Hz, 6H). HRMS (ESI): $[M + H]^+$ calcd for $C_{24}H_{30}N_2O_2$, 379.2380; found, 379.2382.

*8-Cyclopentyl-6-(3,6,6-trimethyl-4-oxo-4,5,6,7-tetrahydro-1H-indol-1-yl)-3,4-dihydroisoquinolin-1(2H)-one (**31**).* Yield 48%. ^{1}H NMR (400 MHz, DMSO-d_6) δ δ 8.03 (s, 1H), 7.26 (d, J = 2.0 Hz, 1H), 7.21 (d, J = 2.0 Hz, 1H), 6.88 (s, 1H), 4.46−4.17 (m, 1H), 3.3−3.22 (m, 2H), 2.92−2.88 (m, 2H), 2.76−2.71 (m, 2H), 2.26 (s, 2H), 2.22 (s, 3H), 2.04−1.99 (m, 2H), 1.82−1.76 (m, 2H), 1.65−1.50 (m, 4H), 0.99 (s, 6H). ^{13}C NMR (100 MHz, DMSO-d_6) δ 193.60, 164.55, 149.95, 142.13, 141.47, 139.62, 126.81, 121.18, 120.81, 120.30, 118.66, 118.37, 51.95, 36.61, 35.07, 34.55, 30.05, 27.93, 25.32, 11.25. HRMS (ESI): $[M + H]^+$ calcd for $C_{25}H_{30}N_2O_2$, 391.2380; found, 391.2376.

*8-Cyclohexyl-6-(3,6,6-trimethyl-4-oxo-4,5,6,7-tetrahydro-1H-indol-1-yl)-3,4-dihydroisoquinolin-1(2H)-one (**32**).* Yield 67%. ^{1}H NMR (400 MHz, DMSO-d_6) δ 8.02−7.98 (m, 1H), 7.25 (s, 1H), 7.22 (s, 1H), 6.87 (s, 1H), 4.08−3.95 (m, 1H), 3.31−3.24 (m, 2H), 2.93−2.88 (m, 2H), 2.77−2.70 (m, 2H), 2.26 (s, 2H), 2.22 (s, 3H), 1.83−1.67 (m, 5H), 1.55−1.11 (m, 5H), 0.99 (s, 6H). HRMS (ESI): $[M + H]^+$ calcd for $C_{26}H_{32}N_2O_2$, 405.2537; found, 405.2540.

*8-(Tetrahydro-2H-pyran-4-yl)-6-(3,6,6-trimethyl-4-oxo-4,5,6,7-tetrahydro-1H-indol-1-yl)-3,4-dihydroisoquinolin-1(2H)-one (**33**).* Yield 42%. ^{1}H NMR (400 MHz, DMSO-d_6) δ 8.05 (s, 1H), 7.29−7.26 (m, 2H), 6.91 (s, 1H), 4.30−4.20 (m, 1H), 3.94 (d, J = 10.7 Hz, 2H), 3.46−3.37 (m, 2H), 3.32−3.27 (m, 2H), 2.95−2.86 (m, 2H), 2.75−2.73 (m, 2H), 2.26 (s, 2H), 2.22 (s, 3H), 1.75−1.54 (m, 4H), 1.00 (s, 6H). HRMS (ESI): $[M + H]^+$ calcd for $C_{25}H_{30}N_2O_3$, 407.2329; found, 407.2331.

*8-Cyclobutyl-6-(3,6,6-trimethyl-4-oxo-4,5,6,7-tetrahydro-1H-indol-1-yl)-3,4-dihydroisoquinolin-1(2H)-one (**34**).* Yield 62%. ^{1}H NMR (400 MHz, DMSO-d_6) δ 7.98 (s, 1H), 7.26 (s, 1H), 7.24 (s, 1H), 6.91 (s, 1H), 4.60−4.49 (m, 1H), 3.32−3.23 (m, 2H), 2.89 (t, J = 6.2 Hz, 2H), 2.74 (s, 2H), 2.35−2.26 (m, 2H), 2.26 (s 2H), 2.23 (s, 3H), 2.10−1.97 (m, 2H), 1.96−1.86 (m, 1H), 1.79−1.70 (m, 1H), 1.00 (s, 6H). HRMS (ESI): $[M + H]^+$ calcd for $C_{24}H_{28}N_2O_2$, 377.2224; found, 377.2228.

*8-Butyl-6-(3,6,6-trimethyl-4-oxo-4,5,6,7-tetrahydro-1H-indol-1-yl)-3,4-dihydroisoquinolin-1(2H)-one (**35**).* Yield 43%. ^{1}H NMR (500 MHz, DMSO-d_6) δ 7.94 (s, 1H), 7.22 (s, 1H), 7.16 (s, 1H), 6.86 (s, 1H), 3.13−3.07 (m, 2H), 2.90 (t, J = 6.0 Hz, 2H), 2.72 (s, 2H), 2.55 (s, 2H), 2.26 (s, 2H), 2.21 (s, 3H), 1.59−1.47 (m, 2H), 1.37−1.27 (m, 2H), 0.99 (s, 6H), 0.88 (t, J = 7.3 Hz, 3H). HRMS (ESI): $[M + H]^+$ calcd for $C_{24}H_{30}N_2O_2$, 379.2380; found, 379.2378.

*8-(tert-Butyl)-6-(3,6,6-trimethyl-4-oxo-4,5,6,7-tetrahydro-1H-indol-1-yl)-3,4-dihydroisoquinolin-1(2H)-one (**36**).* Yield 72%. ^{1}H NMR (400 MHz, DMSO-d_6) δ 8.12 (s, 1H), 7.37 (s, 1H), 7.26 (s,1H),

dx.doi.org/10.1021/jm500042s | J. Med. Chem. 2014, 57, 3382−3400

6.87 (s,1H), 3.24 (dd, J = 11.2, 5.4 Hz, 2H), 2.87 (t, J = 5.4 Hz, 2H), 2.73 (s, 2H), 2.27 (s, 2H), 2.23 (s, 3H), 1.49 (s, 9H), 1.01 (s, 6H). HRMS (ESI): $[M + H]^+$ calcd for $C_{24}H_{30}N_2O_2$, 379.2380; found, 379.2381.

*8-Benzyl-6-(3,6,6-trimethyl-4-oxo-4,5,6,7-tetrahydro-1H-indol-1-yl)-3,4-dihydroisoquinolin-1(2H)-one (**37**).* Yield 45%. ^{1}H NMR (400 MHz, DMSO-d_6) δ 7.88 (s, 1H), 7.35−7.28 (m, 5H), 7.26−7.17 (m, 1H), 7.06 (s, 1H), 6.47 (s, 1H), 4.01 (s, 2H), 3.41−3.28 (m, 2H), 2.94−2.88 (m, 2H), 2.25 (s, 2H), 2.19−2.10 (m, 5H), 0.96 (s, 3H), 0.93 (s, 3H). ^{13}C NMR (100 MHz, DMSO-d_6) δ 193.15, 161.93, 145.57, 143.41, 142.04, 140.07, 137.40, 128.83, 128.57, 127.93, 127.50, 126.19, 123.72, 121.74, 117.08, 116.41, 52.22, 35.56, 34.95, 29.28, 28.25, 28.01, 11.34. HRMS (ESI): $[M + H]^+$ calcd for $C_{27}H_{28}N_2O_2$, 413.2224; found, 413.2229.

*8-Phenyl-6-(3,6,6-trimethyl-4-oxo-4,5,6,7-tetrahydro-1H-indol-1-yl)-3,4-dihydroisoquinolin-1(2H)-one (**38**).* Yield 64%. ^{1}H NMR (500 MHz, DMSO-d_6) δ 7.94 (s, 1H), 7.41 (s, 1H), 7.39−7.23 (m, 5H), 7.14 (d, J = 1.7 Hz, 1H), 6.93 (s, 1H), 2.98 (t, J = 5.9 Hz, 2H), 2.75 (s, 2H), 2.55 (s, 2H), 2.25 (s, 2H), 2.20 (s, 3H), 0.99 (s, 6H). HRMS (ESI): $[M + H]^+$ calcd for $C_{26}H_{26}N_2O_2$, 399.2067; found, 399.2067.

*8-(4-Fluorophenyl)-6-(3,6,6-trimethyl-4-oxo-4,5,6,7-tetrahydro-1H-indol-1-yl)-3,4-dihydroisoquinolin-1(2H)-one (**39**).* Yield 73%. ^{1}H NMR (500 MHz, DMSO-d_6) δ 7.95 (d, J = 14.1 Hz, 1H), 7.41 (d, J = 1.7 Hz, 1H), 7.33 (dd, J = 8.6, 5.5 Hz, 2H), 7.26−7.07 (m, 3H), 6.92 (s, 1H), 3.42−3.38 (m, 2H), 2.97 (t, J = 6.0 Hz, 2H), 2.74 (s, 2H), 2.24 (s, 2H), 2.20 (s, 3H), 0.98 (s, 6H). HRMS (ESI): $[M + H]^+$ calcd for $C_{26}H_{25}FN_2O_2$, 417.1973; found, 417.1975.

*8-(3-Fluorophenyl)-6-(3,6,6-trimethyl-4-oxo-4,5,6,7-tetrahydro-1H-indol-1-yl)-3,4-dihydroisoquinolin-1(2H)-one (**40**).* Yield 59%. ^{1}H NMR (500 MHz, DMSO-d_6) δ 7.98 (s, 1H), 7.44 (s, 1H), 7.44−7.39 (m, 1H), 7.23−7.10 (m, 4H), 6.94 (s, 1H), 2.98 (t, J = 6.1 Hz, 2H), 2.76 (s, 2H), 2.55 (s, 2H), 2.25 (s, 2H), 2.20 (s, 3H), 0.99 (s, 6H). HRMS (ESI): $[M + H]^+$ calcd for $C_{26}H_{25}FN_2O_2$, 417.1973; found, 417.1976.

*8-(4-Methoxyphenyl)-6-(3,6,6-trimethyl-4-oxo-4,5,6,7-tetrahydro-1H-indol-1-yl)-3,4-dihydroisoquinolin-1(2H)-one (**41**).* Yield 61%. ^{1}H NMR (400 MHz, DMSO-d_6) δ 7.93 (s, 1H), 7.38 (d, J = 2.1 Hz, 1H), 7.33−7.20 (m, 2H), 7.14 (d, J = 2.2 Hz, 1H), 7.04−6.85 (m, 3H), 3.79 (s, 3H), 3.48−3.40 (m, 2H), 2.97 (t, J = 6.0 Hz, 2H), 2.76 (s, 2H), 2.26 (s, 2H), 2.22 (s, 3H), 1.01 (s, 6H). ^{13}C NMR (100 MHz, DMSO-d_6) δ 193.55, 163.38, 158.20, 143.84, 143.07, 141.63, 139.21, 133.46, 129.72, 126.75, 125.00, 121.48, 120.98, 118.73, 118.37, 112.99, 55.02, 52.01, 36.50, 35.17, 29.86, 27.95, 11.28. HRMS (ESI): $[M + H]^+$ calcd for $C_{27}H_{28}N_2O_3$, 429.1729; found, 429.2173.

3-((4-Chloropyridin-3-yl)amino)-5,5-dimethylcyclohex-2-enone (48). A stirring mixture of 4-chloropyridin-3-amine **45** (1.0 g, 7.8 mmol), 5,5-dimethylcyclohexane-1,3-dione (3.3 g, 23.3 mmol), and p-TsOH-H_2O (150 mg, 0.78 mmol) in toluene (100 mL) was heated at reflux for 3 h using a Dean−Stark apparatus to remove water. The cooled solution was partitioned between DCM (500 mL) and saturated aq $NaHCO_3$ solution (300 mL). The organic portion was evaporated to dryness under reduced pressure. The residue was purified via silica gel chromatography using 5% MeOH in DCM to obtain the desired product (530 mg, 2.12 mmol, yield 27%). ^{1}H NMR (400 MHz, $CDCl_3$) δ 8.62 (s, 1H), 8.35 (d, J = 5.2 Hz, 1H), 7.40 (d, J = 5.2 Hz, 1H), 6.08 (s, 1H), 5.39 (s, 1H), 2.61 (s, 2H), 2.26 (s, 2H), 1.09 (s, 6H).

3-((3-Bromopyridin-2-yl)amino)-5,5-dimethylcyclohex-2-enone (49). A stirring solution of 2-amino-3-bromopyridine **46** (10 g, 57.8 mmol), 5,5-dimethyl-1,3-cyclohexanedione (24.3 g, 173.4 mmol), p-TsOH-H_2O (1.1 g, 5.78 mmol), and toluene (400 mL) was heated at reflux under N_2 for 20 h using a Dean−Stark apparatus to remove water. The reaction mixture was concentrated under reduced pressure. The residue was dissolved in DCM (1 L) and washed with saturated aq $NaHCO_3$ solution (500 mL). The organic portion was removed and washed with saturated aq $NaHCO_3$ solution (3 × 500 mL), water (500 mL), and saturated aq NaCl solution (500 mL). The organic portion was dried over Na_2SO_4 and filtered. The filtrate was concentrated under reduced pressure, and the residue was purified by silica gel chromatography using 5−40% EtOAc in hexanes to give a yellow solid (7.0 g, 32.7 mmol, yield 41%). LCMS (C18 column eluting with 1−99% ACN/water gradient over 3 min with TFA modifier) M + 1: 295.5 (1.20 min). ^{1}H NMR (400 MHz, DMSO-d_6) δ 8.48−8.25 (m, 2H), 8.10 (dd, J = 7.9, 1.6 Hz, 1H), 7.06 (dd, J = 7.9, 4.7 Hz, 1H), 6.21 (s, 1H), 2.52 (s, 2H), 2.10 (s, 2H), 1.03 (s, 6H).

7,7-Dimethyl-7,8-dihydro-5*H*-pyrido[3,2-*b*]indol-9(6*H*)-one (50). A stirring solution of 2-chloropyridin-3-amine **44** (2.0 g, 15.6 mmol), 5,5-dimethylcyclohexane-1,3-dione (2.8 g, 20.2 mmol), p-TsOH-H_2O (20 mg, 0.11 mmol), and toluene (50 mL) was heated at reflux for 24 h. The reaction was cooled and added to 50 mL of aq $NaHCO_3$ solution. The mixture was extracted with DCM (3 × 50 mL). The organic fractions were combined, dried ($MgSO_4$), filtered, and concentrated under reduced pressure to yield 3-((2-chloropyridin-3-yl)amino)-5,5-dimethylcyclohex-2-enone **47** (3.9 g, 15.6 mmol, yield 100%) as a white solid. A portion of the obtained 3-((2-chloropyridin-3-yl)amino)-5,5-dimethylcyclohex-2-enone **47** (700 mg, 2.79 mmol) was combined with Cs_2CO_3 (2.73 g, 8.38 mmol), $Pd(PPh_3)_4$ (322 mg, 0.28 mmol), and DMF (5 mL) and heated at 150 °C for 2 h. The reaction mixture was cooled and diluted with DCM. The mixture was passed through a short plug of silica gel (3 g) using DCM, and the eluent was concentrated under reduced pressure to give a white solid (455 mg, 2.13 mmol, yield 76%). ^{1}H NMR (400 MHz, DMSO-d_6) δ 13.60 (s, 1H), 8.62 (d, J = 7.8 Hz, 1H), 8.53 (d, J = 5.7 Hz, 1H), 7.73 (dd, J = 8.1, 6.0 Hz, 1H), 3.09 (s, 2H), 2.53 (s, 2H), 1.12 (d, J = 12.5 Hz, 6H).

7,7-Dimethyl-6,7,8,9-tetrahydro-5*H*-pyrido[3,4-*b*]indol-5-one (51). A microwave vessel was loaded with 3-[(4-chloro-3-pyridyl)amino]-5,5-dimethyl-cyclohex-2-en-1-one **48** (400 mg, 1.60 mmol), $Pd(PPh_3)_4$ (369 mg, 0.32 mmol), and Cs_2CO_3 (1.60 g, 4.8 mmol). The vessel was purged with N_2 and heated at 150 °C for 6 min via microwave irradiation. The mixture was diluted with MeOH (5 mL) and DCM (100 mL) and filtered. The filtrate was evaporated to dryness under reduced pressure. The residue was purified via silica gel chromatography using 10% MeOH in DCM to obtain a light-yellow solid (300 mg, 1.40 mmol, yield 88%). ^{1}H NMR (400 MHz, DMSO-d_6) δ 12.29 (s, 1H), 8.74 (s, 1H), 8.25 (d, J = 5.3 Hz, 1H), 7.82 (d, J = 5.3 Hz, 1H), 2.91 (s, 2H), 2.37 (s, 2H), 1.09 (s, 6H).

7,7-Dimethyl-6,7,8,9-tetrahydro-5*H*-pyrido[2,3-*b*]indol-5-one (52). A stirring mixture of 3-(3-bromopyridin-2-ylamino)-5,5-dimethylcyclohex-2-enone **49** (5.0 g, 16.9 mmol), $Pd(PPh_3)_4$ (980 mg, 0.85 mmol), Cs_2CO_3 (8.3 g, 25.4 mmol), and DMF (20 mL) was heated at 150 °C for 3 h. The reaction mixture was filtered through a pad of Celite, and the filter cake was washed with DCM (50 mL). The filtrate was washed with saturated aq NaCl solution (150 mL), dried over Na_2SO_4 (250 g), and concentrated under reduced pressure. The residue was a purified by silica gel chromatography using 5% MeOH in DCM to give a tan solid (1.3 g, yield 36%). ^{1}H NMR (400 MHz, DMSO-d_6) δ 12.36 (s, 1H), 8.22 (ddd, J = 9.4, 6.3, 1.6 Hz, 2H), 7.19 (dd, J = 7.7, 4.8 Hz, 1H), 2.88 (s, 2H), 2.36 (s, 2H), 1.10 (s, 6H).

2,2-Dimethyl-2,3,5,6,7,8-hexahydro-1*H*-carbazol-4(9*H*)-one (54). To a stirring solution of 2*E*)-2-hydroxyiminocyclohexanone **53** (50 mg, 0.39 mmol), 5,5-dimethylcyclohexane-1,3-dione (55 mg, 0.39 mmol), AcOH (2.8 mL), and H_2O (1.2 mL) was added Zn powder (51 mg, 0.79 mmol). The mixture was heated at 80 °C for 19 h. The mixture was added to H_2O (50 mL) and neutralized to pH 7 with saturated aq $NaHCO_3$. The mixture was extracted with EtOAc (2 × 20 mL), and the organic fractions were combined, dried ($MgSO_4$), filtered, and concentrated under reduced pressure. The residual oil was purified via silica gel chromatography using 10−70% EtOAc in hexanes to yield the desired product as a white solid (25 mg, 0.12 mmol, yield 29%). ^{1}H NMR (400 MHz, MeOD) δ 2.64 (d, J = 2.8 Hz, 4H), 2.52 (s, 2H), 2.27 (s, 2H), 1.79 (dd, J = 17.4, 11.6 Hz, 4H), 1.11 (s, 6H).

2,7,7-Trimethyl-3,4,6,7,8,9-hexahydro-1*H*-pyrido[3,4-*b*]-indol-5(2*H*)-one (59). To a stirring solution of 2,2-dimethoxy-*N*-methyl-ethanamine **56** (18.1 g, 19.5 mL, 152.1 mmol) and AcOH (60 mL), under N_2, at rt was added 37% formaldehyde in water (12.3 g, 11.3 mL, 152.1 mmol). The solution was stirred at rt for 10 min. This solution was then added dropwise to a stirring solution of 6,6-dimethyl-5,7-dihydro-1*H*-indol-4-one **55** (25 g, 152.1 mmol) and AcOH (250 mL) over a period of 30 min. The solution was then

stirred at rt for 24 h. The solution was partitioned between water (700 mL) and Et_2O (50 mL). The aqueous portion was carefully neutralized with 30% aq NH_4OH solution and extracted with DCM (4 × 200 mL). The organic portions were combined, dried (Na_2SO_4), and evaporated to dryness. The brown oil was purified by silica gel chromatography using 5% MeOH in DCM to obtain the acetal intermediate as a yellow oil (37.0 g). The acetal intermediate was added to aq HCl (170 mL of 8 M, 1.4 mol) and was heated at 70 °C for 5 min. The solution was quickly cooled to 25 °C and injected via syringe into a N_2 purged vessel containing Pd on C (36.2 g, 33.9 mmol) and EtOH (200.0 mL). The mixture was shaken at 25 °C for 24 h under 1 atm of H_2 at 30 psi using a Parr apparatus. The solution was filtered through a bed of Celite, and the filtrate was concentrated under reduced pressure. The residual oil was dissolved in water (100 mL) and basified to pH 10 using 30% aq NH_4OH. The precipitate was filtered, washed with water (20 mL), and vacuum-dried to obtain the desired compound as a white solid (5.1 g, 21.9 mmol, yield 14%). ^{1}H NMR (400 MHz, DMSO-d_6) δ 10.93 (s, 1H), 2.66−2.52 (m, 5H), 2.50 (dd, J = 3.6, 1.8 Hz, 3H), 2.34 (s, 3H), 2.14 (s, 2H), 1.03 (d, J = 9.9 Hz, 6H).

7,7-Dimethyl-3,4,6,7,8,9-hexahydro-1*H*-pyrido[3,4-*b*]indol-5(2*H*)-one (61). To a stirring solution of *N*-benzyl-2,2-dimethoxyethanamine **58** (29.7 g, 152.1 mmol) and AcOH (60 mL), under N_2, at rt was added formaldehyde (12.3 g, 11.3 mL, 152.1 mmol, 37% solution in water). The solution was stirred at rt for 10 min. This solution was then added dropwise to a stirring solution of 6,6-dimethyl-5,7-dihydro-1*H*-indol-4-one **55** (25.0 g, 152.1 mmol) and AcOH (250 mL) over a period of 30 min. The solution was then stirred at rt for 19 h. The solution was concentrated under reduced pressure. The residue was carefully neutralized with saturated aq $NaHCO_3$ solution and extracted with DCM (3 × 200 mL). The organic portions were combined, dried (Na_2SO_4), and evaporated under reduced pressure to give a yellow oil. The oil was purified by silica gel chromatography using 50% EtOAc in hexanes to obtain a semipure oil. The obtained oil was dissolved in EtOAc (300 mL), and to this solution was added Et_2O (200 mL). The formed precipitate was filtered and vacuum-dried to obtain the intermediate acetal as a white solid (44 g). The acetal intermediate was dissolved in aq HCl (455 mL of 8 M, 3.64 mmol) and heated at 70 °C for 15 min. The solution was quickly cooled to 25 °C and injected via syringe into a N_2 purged vessel containing 10% Pd on C (43.1 g, 40.5 mmol) and EtOH (450 mL). The mixture was shaken at 25 °C for 20 h under H_2 at 16 psi using a Parr apparatus. The solution was filtered through a bed of Celite, and the filtrate was concentrated under reduced pressure. The residual oil was dissolved in water (100 mL) and basified to pH 10 using 30% aq NH_4OH. The solution was extracted with DCM (8 × 100 mL). The organic portions were combined, dried (Na_2SO_4), and concentrated under reduced pressure. The residual solid was triturated with Et_2O (100 mL), and the resulting white solid was dried under vacuum (8.8 g, 40.3 mmol, yield 26%). ^{1}H NMR (400 MHz, DMSO-d_6) δ 11.40 (s, 1H), 8.75 (bs, 1H), 4.07 (s, 2H), 3.27−3.22 (m, 2H), 2.87−2.79 (m, 2H), 2.62 (s, 2H), 2.19 (s, 2H), 1.02 (s, 6H).

***tert*-Butyl 7,7-Dimethyl-9-*oxo*-3,4,6,7,8,9-hexahydro-1*H*-pyrido[4,3-*b*]indole-2(5*H*)-carboxylate (62).** To a stirring suspension of 7,7-dimethyl-2,3,4,6,8,9-hexahydro-1*H*-pyrido[3,4-*b*]indol-5-one **61** (1.0 g, 4.581 mmol) and DCM (20.00 mL), under N_2, at rt was added Et_3N (556 mg, 766 μL, 5.50 mmol) and di-*tert*-butyl dicarbonate (1.2 g, 1.3 mL, 5.50 mmol). The mixture was stirred at rt for 30 min. The mixture was diluted with MeOH (5 mL) and directly purified via silica gel chromatography using 5% MeOH in DCM to obtain a white solid (1.2g, 3.77 mmol, yield 82%). ^{1}H NMR (400 MHz, DMSO-d_6) δ 11.06 (s, 1H), 4.31 (s, 2H), 3.50 (t, J = 5.7 Hz, 2H), 3.32 (s, 2H), 2.58 (s, 2H), 2.15 (s, 2H), 1.41 (s, 9H), 1.02 (s, 6H).

(*S*)-4-Bromo-2-fluoro-6-((tetrahydrofuran-3-yl)amino)-benzamide (64). To a stirring solution of 4-bromo-2,6-difluorobenzonitrile **63** (7.4 g, 33.7 mmol) in DMSO (74 mL) was added DIEA (10.5 g, 14.1 mL, 80.9 mmol), followed by the addition of (*S*)-tetrahydrofuran-3-amine hydrochloride (5.0 g, 40.5 mmol) under N_2. The mixture was stirred at rt for 19 h. The solution was partitioned between Et_2O (250 mL) and water (350 mL). The organic layer was evaporated to dryness under reduced pressure, and the residue was purified via silica gel chromatography using 30% EtOAc in hexanes to give a white solid (7.9 g, 27.7 mmol, yield 82%). ^{1}H NMR (400 MHz, DMSO) δ 7.00−6.85 (m, 2H), 6.78 (d, J = 6.2 Hz, 1H), 4.32−4.15 (m, 1H), 3.92−3.83 (m 2H), 3.76−3.68 (m, 1H), 3.69−3.62 (m, 1H), 2.33−2.09 (m, 1H), 2.04−1.77 (m, 1H).

2-Bromo-4-(2,7,7-trimethyl-5-*oxo*-3,4,5,6,7,8-hexahydro-1*H*-pyrido[3,4-*b*]indol-9(2*H*)yl)benzonitrile (65). 2,7,7-trimethyl-1,3,4,6,8,9-hexahydropyrido[3,4-*b*]indol-5-one **59** (750 mg, 3.23 mmol) was dissolved in DMF (7.5 mL), and to it was added NaH (258 mg, 6.46 mmol, 60% in mineral oil). The mixture was allowed to stir for 5 min. To this mixture was added 2-bromo-4-fluorobenzonitrile (1.6 g, 8.1 mmol), and the mixture was stirred at 150 °C for 10 min. The reaction was cooled and purified by silica gel chromatography using 20% MeOH in DCM to afford a white solid (970 mg, 2.35 mmol, yield 73%). ^{1}H NMR (400 MHz, DMSO-d_6) δ 8.13 (d, J = 8.3 Hz, 1H), 8.04 (d, J = 2.0 Hz, 1H), 7.65 (dd, J = 8.3, 2.0 Hz, 1H), 3.21 (s, 2H), 2.76−2 0.71 (m, 2H), 2.61−2.57 (m, 4H), 2.29 (s, 3H), 2.24 (s, 2H), 0.99 (s, 6H).

6,8-Difluoro-3,4-dihydroisoquinolin-1(2*H*)-one (67). To a stirring solution of 5,7-difluoroindan-1-one **66** (10 g, 59.5 mmol) in $MeSO_3H$ (60 mL) at 0 °C was added NaN_3 (4.1 g, 62.4 mmol) in portions over 10 min (exothermic). The mixture was stirred at 0 °C for 30 min, then allowed to warm to rt and stirred for 2 h. The mixture was poured onto ice (150 g), and to this solution was added 1.0N NaOH aq solution until pH 10 was reached. The organic layer was separated and concentrated to a volume of 15 mL. Et_2O (50 mL) was added, and the mixture was filtered and vacuum-dried to give a white solid (5.2 g, 28.4 mmol, yield 48%). ^{1}H NMR (400 MHz, $CDCl_3$) δ 7.28 (d, J = 4.5 Hz, 1H), 6.81 (d, J = 2.4 Hz, 1H), 6.80−6.78 (m, 1H), 6.77 (s, 1H), 3.56−3.48 (m, 2H), 2.97 (dd, J = 12.3, 5.8 Hz, 2H).

(*E*)-2-(2-Cyclopropylvinyl)-4-fluorobenzonitrile (69). A mixture of 2-bromo-4-fluoro-benzonitrile (100 mg, 0.50 mmol), 2-[(*E*)-2-cyclopropylvinyl]-4,4,5,5-tetramethyl-1,3,2-dioxaborolane (97 mg, 104 μL, 0.50 mmol), *tert*-butylamine (110 mg, 157 μL, 1.50 mmol), and Pd(dppf)Cl_2 (37 mg, 0.05 mmol), was taken up in 2-propanol (3.3 mL) and water (1.6 mL). This mixture was stirred at 90 °C under N_2 for 19 h. The mixture was filtered, and the filtrate was concentrated under reduced pressure. The residue was partitioned between EtOAc and water. The aqueous phase was extracted twice with EtOAc. The organic phases were combined, dried ($MgSO_4$), filtered, and concentrated under reduced pressure. The residue was purified by silica gel chromatography with 0−100% EtOAc in hexanes to obtain a white solid (67 mg, 0.36 mmol, yield 72%). ^{1}H NMR (400 MHz, $CDCl_3$) δ 7.58 (dd, J = 8.6, 5.6 Hz, 1H), 7.24−7.18 (m, 1H), 6.94 (ddd, J = 8.5, 7.9, 2.5 Hz, 1H), 6.80 (dd, J = 15.6, 1.5 Hz, 1H), 5.92 (dd, J = 15.6, 9.3 Hz, 1H), 1.79−1.61 (m, 1H), 1.01−0.91 (m, 2H), 0.68−0.52 (m, 2H).

■ ASSOCIATED CONTENT

Ⓢ Supporting Information

Analytical data for all compounds and X-ray crystallography information. This material is available free of charge via the Internet at http://pubs.acs.org.

Accession Codes

New protein/ligand coordinates have been deposited in the PDB with codes 4O04, 4O05, 4O07, 4O09, and 4O0B, respectively.

■ AUTHOR INFORMATION

Corresponding Author

*Phone: 858-404-8409. E-mail: Justin_ernst@vrtx.com.

Notes

The authors declare no competing financial interest.

■ ACKNOWLEDGMENTS

The Berkeley Center for Structural Biology is supported in part by the National Institutes of Health, National Institute of General Medical Sciences, and the Howard Hughes Medical Institute. The Advanced Light Source is supported by the Director, Office of Science, Office of Basic Energy Sciences, of the U.S. Department of Energy under contract no. DE-AC02-05CH11231.

■ ABBREVIATIONS USED

HSP90, heat shock protein 90; HD, Huntington's disease; Htt, Huntingtin; mHtt, mutant Huntingtin; CNS, central nervous system; SAR, structure−activity relationship; HOAc, acetic acid; DMF, dimethylformamide; EtOH, ethanol; DMSO, dimethyl sulfoxide; dppf or DPPF, 1,10 bis-(diphenylphosphino)ferrocene; THF, tetrahydrofuran; TFA, trifluoroacetic acid; MsOH, methanesulfonic acid; PBS, phosphate-buffered saline; LCMS or LC-MS, liquid chromatography−mass spectrometry; HPLC, high pressure liquid chromatography; HRMS, high-resolution mass spectroscopy

■ REFERENCES

(1) (a) Pratt, W. B.; Toft, D. O. Regulation of Signaling Protein Function and Trafficking by the hsp90/hsp70-Based Chaperone Machinery. *Exp. Biol. Med.* **2003**, *228*, 111−133. (b) Buchner, J. Hsp90 & Co.—a holding for folding. *Trends Biochem. Sci.* **1999**, *24*, 136−141. (c) Young, J.; Moarefi, I.; Hartl, F. U. Hsp90: a specialized but essential protein folding tool. *J. Cell. Biol.* **2001**, *154*, 267−274. (d) Picard, D. Heat-shock protein 90, a chaperone for folding and regulation. *Cell. Mol. Life Sci.* **2002**, *59*, 1640−1648. (e) Mosser, D. D.; Morimoto, R. I. Molecular chaperones and the stress of oncogenesis. *Oncogene* **2004**, *23*, 2907−2918. (f) Young, J. C.; Agashe, V. R.; Siegers, K.; Hartl, F. U. Pathways of chaperone-mediated protein folding in the cytosol. *Nature Rev. Mol. Cell Biol.* **2004**, *5*, 781−789.

(2) Biamonte, M. A.; Van de Water, R.; Arndt, J. W.; Scannevin, R. H.; Perret, D.; Lee, W-C. Heat Shock Protein 90: Inhibitors in Clinical Trials. *J. Med. Chem.* **2010**, *53*, 3−17.

(3) (a) Grenert, J. P.; Sullivan, W. P.; Fadden, P.; Haystad, T. A.; Clark, J.; Mimmaugh, E.; Krutzsch, H.; Ochel, H. J.; Schulte, T. W.; Sausville, E; Neckers, L. M.; Toft, D. O. The amino terminal domain of the heat shock protein 90 (hsp90) that binds geldanamycin is an ATP/ADP switch domain that regulates hsp90 conformation. *J. Biol. Chem.* **1997**, *272*, 23843−23850. (b) Grenert, J. P.; Johnson, B. D.; Toft, D. O. The importance of ATP binding and hydrolysis by hsp90 in formation and function of protein heterocomplexes. *J. Biol. Chem.* **1999**, *274*, 17525−17533. (c) Pearl, L. H.; Prodromou, C. Structure, function, and mechanism of the Hsp90 molecular chaperone. *Adv. Protein Chem.* **2001**, *59*, 157−186. (d) Prodromou, C.; Pearl, L. H. Structure and functional relationship of the Hsp90. *Curr. Cancer Drug Targets* **2003**, *3*, 301−323.

(4) Ernst, J. T.; Liu, M.; Zuccola, H.; Neubert, T.; Beaumont, K.; Turnbull, A.; Kallel, A.; Stamos, D. Correlation between chemotype-dependent binding conformations of HSP90α/β and isoform selectivity—implications for the structure-based design of HSP90α/β selective inhibitors for treating neurodegenerative diseases. *Bioorg. Med. Chem. Lett.* **2014**, *24*, 204−208.

(5) Sreedhar, A. S.; Kalmar, E.; Csermely, P.; Shen, Y-F. HSP90 isoforms: functions, expression and clinical importance. *FEBS Lett.* **2004**, *562*, 11−15.

(6) Baldo, B.; Weiss, A.; Parker, C. N.; Bibel, M.; Paganetti, P.; Kaupmann, K. A Screen for Enhancers of Clearance Identifies Huntingtin as a Heat Shock Protein 90 (Hsp90) Client Protein. *J. Biol. Chem.* **2012**, *287*, 1406−1414.

(7) (a) Gusella, J. F.; Wexler, N. S.; Conneally, P. M.; Naylor, S. L.; Anderson, M. A.; Tanzi, R. E. A polymorphic DNA marker genetically linked to Huntington's disease. *Nature* **1983**, *306*, 234−238. (b) Mac Donald, M. E.; et al. A novel gene containing a trinucleotide repeat that is expanded and unstable on Huntington's disease chromosomes. The Huntington's Disease Collaborative Research Group. *Cell* **1993**, *72*, 971−983. (c) Rubinsztein, D. C.; Leggo, J.; Coles, R.; Almqvist, E.; Biancalana, V.; Cassiman, J. J. Phenotypic characterization of individuals with 30−40 CAG repeats in the Huntington disease (HD) gene reveals HD cases with 36 repeats and apparently normal elderly individuals with 36−39 repeats. *Am. J. Hum. Genet.* **1996**, *59*, 16−22.

(8) Putcha, P.; Danzer, K. M.; Kranich, L. R.; Scott, A.; Silinski, S. M.; Hicks, C. D.; Veal, J. M.; Steed, P. M.; Hyman, B. T.; McLean, P. J. Brain Permeable Small-Molecule Inhibitors of Hsp90 Prevent α-Synuclein Oligomer Formation and Rescue α-Synuclein-Induced Toxicity. *J. Pharm. Exp. Ther.* **2010**, *332*, 849−857.

(9) Brough, P. A.; Aherne, W.; Barril, X.; Borgognoni, J.; Boxall, K.; Cansfield, J. E.; Cheung, K. M.; Collins, I.; Davies, N. G.; Drysdale, M. J.; Dymock, B.; Eccles, S. A.; Finch, H.; Fink, A.; Hayes, A.; Howes, R.; Hubbard, R. E.; James, K.; Jordan, A. M.; Lockie, A.; Martins, V.; Massey, A.; Matthews, T. P.; McDonald, E.; Northfield, C. J.; Pearl, L. H.; Prodromou, C.; Ray, S.; Raynaud, F. I.; Roughley, S. D.; Sharp, S. Y.; Surgenor, A.; Walmsley, D. L.; Webb, P.; Wood, M.; Workman, P.; Wright, L. 4,5-Diarylisoxazole Hsp90 Chaperone Inhibitors: Potential Therapeutic Agents for the Treatment of Cancer. *J. Med. Chem.* **2008**, *51*, 196−218.

(10) Huang, K. H.; Veal, J. M.; Fadden, R. P.; Rice, J. W.; Eaves, J.; Strachan, J.-P.; Barabasz, A. F.; Foley, B. E.; Barta, T. E.; Ma, W.; Silinski, M. A.; Hu, M.; Partridge, J. M.; Scott, A.; DuBois, L. G.; Freed, T.; Steed, P. M.; Ommen, A. J.; Smith, E. D.; Hughes, P. F.; Woodward, A. R.; Hanson, G. J.; McCall, W. S.; Markworth, C. J.; Hinkley, L.; Jenks, M.; Geng, L.; Lewis, M.; Otto, J.; Pronk, B.; Verleysen, K.; Hall, S. E. Discovery of novel 2-aminobenzamide inhibitors of heat shock protein 90 as potent, selective and orally active antitumor agents. *J. Med. Chem.* **2009**, *52*, 4288−4305.

(11) Polli, J. W.; Wring, S. A.; Humphreys, J. E.; Huang, L.; Morgan, J. B.; Webster, L. O.; Serabjit-Singh, C. S. Rational use of in vitro P-glycoprotein assays in drug discovery. *J. Pharmacol. Exp. Ther.* **2001**, *299*, 620−628.

(12) (a) Fernandez, A.; Crespo, A. Protein wrapping: a molecular marker for association, aggregation and drug design. *Chem. Soc. Rev.* **2008**, *37*, 2373−2382. (b) Schmidtke, P.; Luque, F. J.; Murray, J. B.; Barril, X. Shielded Hydrogen Bonds as Structural Determinants of Binding Kinetics: Application in Drug Design. *J. Am. Chem. Soc.* **2011**, *133*, 18903−18910.

(13) (a) Mizuno, M.; Mizufune, H.; Sera, M.; Mineno, M.; Ueda, T. PCT Int. Appl. 2008016184, 2008. (b) Lachance, N.; April, M.; Joly, M-A. Rapid and Efficient Microwave-Assisted Synthesis of 4-, 5-, 6- and 7-Azaindoles Synthesis. *Synthesis* **2005**, *15*, 2571−2577.

(14) Wu, S.; Fluxe, A.; Janusz, J. M.; Sheffer, J. B.; Browning, G.; Blass, B.; Cobum, K.; Hedges, R.; Murawsky, M.; Fang, B.; Fadayel, G. M.; Hare, M.; Djandjighian, L. Discovery and synthesis of tetrahyroindolone derived semicarbazones as selective Kv1.5 blockers. *Bioorg. Med. Chem. Lett.* **2006**, *16*, 5859−5863.

(15) Bobbit, J. M.; Kulkarni, C. L.; Dutta, C. P.; KoFod, H.; Chiong, K. N. Synthesis of Indoles and Carbolines via Aminoacetaldehyde Acetals. *J. Org. Chem.* **1978**, *43*, 3541−3544.

(16) Nikolovska-Coleska, Z.; Wang, R.; Fang, X.; Pan, H.; Tomita, Y.; Li, P.; Roller, P. P.; Krajewski, K.; Saito, N. G.; Stuckey, J. A.; Wang, S. Development and optimization of a binding assay for the XIAP BIR3 domain using fluorescence polarization. *Anal. Biochem.* **2004**, *332*, 261−273.